The ankle joint of *Pterodaustro guinazui*

ROMAIN BURLOT, LAURA CODORNIÚ, LENNA DEFEND, and MICHEL LAURIN

Burlot, R., Codorniú, L., Defend, L., and Laurin, M. 2024. The ankle joint of *Pterodaustro guinazui*. *Acta Palaeontologica Polonica* 69 (2): 329–350.

The hindlimb of pterosaurs has been much less studied than the pterosaur wing. However, it is relevant to understand the evolution, phylogeny and ecology of these animals. This study provides the first complete and detailed description of the ankle of *Pterodaustro guinazui*. It documents three ontogenetic stages observed for the fusion of the tibiotarsus: in the youngest specimens the proximal tarsals are not fused to the tibia; in the subadults the tibiotarsus is formed, but with the suture still visible; in the adults, the tibiotarsus is entirely formed, without any suture. The fusion between astragalus and calcaneum precedes tibiotarsal fusion, but in close succession. The medial condyle of the tibiotarsus is made up of the astragalus, and the lateral condyle is composed of the calcaneum and part of the astragalus. The distal tibiotarsus has three articular facets, the most medial of which seems to greatly restrict the flexion-extension movement, a feature atypical of pterosaurs. The lateral part of the distal tibiotarsus, on the contrary, allows a very wide range of movement. *Pterodaustro guinazui* seems to have had an asymmetrical ankle joint, which could facilitate movements linked to wading behavior. We describe juvenile specimens that retain discrete distal tarsals II and III (common in the "non-pterodactyloid" pterosaurs), but also more mature specimens with completely fused distal tarsals II and III (a condition always observed in the late pterodactyloids). Moreover, the lateral distal tarsal (LDT) appears more robust in *Pterodaustro* than in *Peteinosaurus* or *Dimorphodon*, but shares a waisted shape with these taxa, unlike the more robust shape of the LDT of late pterodactyloids. The new information on the *Pterodaustro* ankle improves our anatomical knowledge of the basal Pterodactyloidea.

Key words: Pterosauria, Pterodactyloidea, *Pterodaustro*, ankle,

Romain Burlot [rom1burlot@gmail.com; ORCID: https://orcid.org/0009-0005-7641-5637], Facultad de Ciencias Físico Matemáticas y Naturales, Dpto. de Geología, Universidad Nacional de San Luis (UNSL), Av. Ejército de Los Andes 950, Bloque II, D5700HHV, San Luis, Argentina. Centre de Recherche en Paléontologie de Paris (CR2P), Museum National d'Histoire Naturelle (MNHN), 43 Rue Buffon, 75005, Paris, France. Consejo Nacional de Investigaciones Científicas y Técnicas (CONICET).
Laura Codorniú [codorniulaura23@gmail.com; ORCID: https://orcid.org/0000-0003-2648-9521], Facultad de Ciencias Físico Matemáticas y Naturales, Dpto. de Geología, Universidad Nacional de San Luis (UNSL), Av. Ejército de Los Andes 950, Bloque II, D5700HHV, San Luis, Argentina. Consejo Nacional de Investigaciones Científicas y Técnicas (CONICET).
Lenna Defend [lenna-defend@hotmail.fr; ORCID: https://orcid.org/0009-0003-4632-3243], Facultad de Ciencias Físico Matemáticas y Naturales, Dpto. de Geología, Universidad Nacional de San Luis (UNSL), Av. Ejército de Los Andes 950, Bloque II, D5700HHV, San Luis, Argentina.
Michel Laurin [michel.laurin@mnhn.fr; ORCID: http://orcid.org/0000-0003-2974-9835], Centre de Recherche en Paléontologie de Paris (CR2P), Museum National d'Histoire Naturelle (MNHN), 43 Rue Buffon, 75005, Paris, France.

Received 31 July 2023, accepted 3 May 2024, published online 26 June 2024.

Introduction

Pterosaurs, a taxon of extinct Mesozoic archosaurs, were the first vertebrates to evolve the ability to fly actively, which required profound physiological and anatomical modifications, especially in their forelimbs (Wellnhofer 1978), which have been widely studied (e.g., Padian 1983; Bennett 2000; Naish et al. 2021; Pittman et al. 2021; Zhou et al. 2022). For example, Kellner (2003) observed that the wing of pterosaurs showed evolutionary trends consisting of an increase of the length of wing metacarpal and pteroid, and a decrease of proportional length of second and third wing phalanges. The hindlimb has been less studied (Wellnhofer 1970, 1974, 1975; Kellner and Tomida 2000; Kellner 2004; Padian 1983, 2008, 2017; Padian et al. 2021), even though abundant, well-preserved material is available for such studies, especially for *Pterodaustro guinazui* from the Loma del *Pterodaustro* site (Albian, Lower Cretaceous of Argentina). This neglect of the hind limb in pterosaur studies may reflect its less spectacular adaptations to flight.

Table 1. Specimens of ankle joints of pterosaurs preserved found in the literature.

Taxa		Publication	Specimen number	Tarsals	
Pterodacyloid status	Genus and species			proximal	distal
“Non-pterodactyloid”	*Anurognathus ammoni*	Bennett 2007	SMNS 81928	tarsal fusion	2?
“Non-pterodactyloid”	*Arcticodactylus cromptonellus*	Jenkins et al. 2001	MGUH VP 3393	unfused	?
“Non-pterodactyloid”	*Austriadraco dallavecchiai*	Dalla-Vecchia 2021	BSP 1994 I 51	total fusion	2?
“Non-pterodactyloid”	*Bellubrunnus rothgaengeri*	Hone et al. 2012	BSP–1993–XVIII–2	unfused	?
“Non-pterodactyloid”	*Campylognathoides liasicus*	Wellnhofer 1974	CM 11424	?	3
“Non-pterodactyloid”	*Carniadactylus rosenfeldi*	Dalla-Vecchia 2009	MFSN 1797	total fusion	2
“Non-pterodactyloid”	*Changchengopterus pani*	Lü 2009	CYGB-0036	unfused	3
“Non-pterodactyloid”	*Darwinopterus linglongtaensis*	Wang et al. 2010	IVPP V16049	total fusion	3?
“Non-pterodactyloid”	*Darwinopterus modularis*	Lü et al. 2010	ZMNH M8782	total fusion	2
“Non-pterodactyloid”	*Darwinopterus robustodens*	Lü et al. 2011	41HIII-0309A	?	?
“Non-pterodactyloid”	*Dendrorynchoides curvidentatus*	Ji and Ji 1998	GMV2128	unfused	?
“Non-pterodactyloid”	*Dimorphodon macronyx*	Padian 1983	YPM350	total fusion	2
“Non-pterodactyloid”	*Dorygnathus banthensis*	Padian 2008	SMNS 55886	?	?
		Padian 2008	SMNS 51827	?	?
“Non-pterodactyloid”	*Douzhanopterus zhengi*	Wang et al. 2017	STM 19–35	total fusion	?
“Non-pterodactyloid”	*Eudimorphodon ranzii*	Dalla-Vecchia 2003	MCSNB 8950	?	3
“Non-pterodactyloid”	*Jeholopterus ningchengensis*	Wang et al. 2002	IVPP V12705	?	?
“Non-pterodactyloid”	*Kunpengopterus antipollicatus*	Zhou et al. 2021	BPMC 0042	?	?
“Non-pterodactyloid”	*Kunpengopterus sinensis*	Wang et al. 2010	IVPP V16047	total fusion	3?
		Cheng et al. 2017	IVPP V 23674	total fusion	2
“Non-pterodactyloid”	*Orientognathus chaoyangensis*	Lü et al. 2015	41HIII-0418	unfused	?
“Non-pterodactyloid”	*Peteinosaurus*? *ranzii*	Dalla-Vecchia 2003	MCSNB 3359	?	2
“Non-pterodactyloid”	*Peteinosaurus zambelii*	Dalla-Vecchia 2003	MCSNB 3496	total fusion	2
“Non-pterodactyloid”	*Preondactylus buffarini*	Dalla-Vecchia 1998	MFSN 1770	?	?
“Non-pterodactyloid”	*Quinglongopterus guoi*	Lü et al. 2012	D3080	unfused	?
“Non-pterodactyloid”	*Raeticodactylus filisurensis*	Stecher 2008	BNM 14524	?	?
“Non-pterodactyloid”	*Rhamphorhychus longicaudus*	Wellnhofer 1975	Exemplar 11	total fusion	2
“Non-pterodactyloid”	*Rhamphorhychus muensteri*	Wellnhofer 1975	Exemplar 68	unfused	3
		Wellnhofer 1975	Exemplar 71	?	3
		Wellnhofer 1975	Exemplar 39	total fusion	3
“Non-pterodactyloid”	*Sinomacrops bondei*	Wei et al. 2021	JPM-2012-001	total fusion	?
“Non-pterodactyloid”	*Sordes pilosus*	Unwin and Bakhurina 1994	PIN 2585	?	?
“Non-pterodactyloid”	*Vesperopterylus lamadongensis*	Lü et al. 2018	BMNHC-PH-001311	total fusion	?
“Non-pterodactyloid”	*Wunkogopterus lii*	Wang et al. 2009	IVPP V15113	total fusion	?
Pterodactyloid	*Aerodactylus scolopaciceps*	Vidovic and Martill 2014	BSP AS V 29	?	?
Pterodactyloid	*Anhanguera piscator*	Kellner and Tomida 2000	NSM-PV-19892	unfused	2
Pterodactyloid	Aurorazhdarchid indet.	Pittman et al. 2022	MB.R.3531a	total fusion	?
Pterodactyloid	*Aurorazhdarcho micronyx*	Winkler 1870; Ösi et al. 2010	ELTE V 256	unfused	2
Pterodactyloid	*Aurorazhdarcho primordius*	Frey 2011	NMB Sh 110	?	?
Pterodactyloid	*Azhdarcho lancicollis*	Averianov 2010	ZIN PH 190/44	total fusion	?
Pterodactyloid	*Balaenognathus maeuseri*	Martill et al. 2023	NKMB P2011-633	unfused	3
Pterodactyloid	*Beipiaopterus chenianus*	Lü 2003	BPM 0002	unfused	?
Pterodactyloid	*Boreopterus cuiae*	Lü and Ji 2005a	JZMP4-07-3	?	?
Pterodactyloid	*Cryodrakon boreas*	Hone et al. 2019	TMP 1992.83	unfused	?
Pterodactyloid	*Ctenochasma elegans*	Wellnhofer 1970	BSP 1875 XIV.501	unfused	3
Pterodactyloid	*Cycnorhamphus suevicus*	Wellnhofer 1970	GPIT 80	?	?
Pterodactyloid	*Elanodactylus prolatus*	Zhou 2010	LPM-R00078	total fusion	2
Pterodactyloid	*Eoazhdarcho liaoxiensis*	Lü and Ji 2005b	GMN-03-11-00	unfused	?
Pterodactyloid	*Eopteranodon yixianensis*	Zhang et al. 2023	IVPP V14190	unfused	?
Pterodactyloid	*Eosipterus yangi*	Ji and Ji 1997	GMV2117	unfused	2?
Pterodactyloid	*Germanodactylus cristatus*	Wellnhofer 1978	SMNK PAL 6592	unfused	?
Pterodactyloid	*Haopterus gracilis*	Wang and Lü 2001	IVPP V 11726	unfused	?
Pterodactyloid	*Huanhepterus quingyangensis*	Dong 1982	IVPP V9070	?	?

Pterodactyloid	*Luchibang xinzhe*	Hone et al. 2020	ELDM 1000	?	?
Pterodactyloid	*Mimodactylus libanensis*	Kellner et al. 2019	MIM F1	?	?
Pterodactyloid	*Muzquizopteryx coahuilensis*	Frey et al. 2006	IGM 8621.	total fusion	2
Pterodactyloid	*Nemicolopterus crypticus*	Wang et al. 2008	IVPP V14377	unfused	1 observable
Pterodactyloid	*Pteranodon* (unspecified)	Bennett 2001a, b	YPM 2462	total fusion	2
Pterodactyloid	*Pterodacylus* sp.	Wellnhofer 1978	BSPG 1936 I50	?	?
Pterodactyloid	*Pterodacylus antiquus*	Wellnhofer 1978	BSPG AS I 739	unfused	2?
Pterodactyloid	*Pterodacylus kochi*	Wellnhofer 1978	AS XIX 3	?	2
Pterodactyloid	*Pterodacylus* (unspecified)	Wellnhofer 1991	?	unfused	3
Pterodactyloid	*Quetzalcoatlus northropi*	Padian 2017	TMM 42138-2	total fusion	2
		Padian 2017	TMM 41954	total fusion	2
Pterodactyloid	*Sinopterus dongi*	Wang and Zhou 2003	IVPP V13363	?	?
		Shen et al. 2021	D3072	unfused	2
Pterodactyloid	*Tapejara* sp.	Kellner 2004	MN 6532-V	unfused	2
Pterodactyloid	*Tethydraco regalis*	Longrich et al. 2018	FSAC-OB 201	unfused	?
Pterodactyloid	*Thanatosdrakon amaru*	David et al. 2022	UNCUYO-LD 307-25	total fusion	?
Pterodactyloid	*Tupandactylus navigans*	Beccari et al. 2021	GP/2E 9266	unfused	2
Pterodactyloid	*Zhejiangopterus linhaiensis*	Cai and Wei 1994	ZMNH M1323	?	?
Pterodactyloid	*Zhenyuanopterus longirostris*	Lü 2010	GLGMV 0001	tarsal fusion	1 observable

The structure of the hindlimbs of birds, the closest flying relatives of pterosaurs, reflects their locomotion, adaptations to swimming, tree climbing, walking, etc. (Abourachid and Höfling 2012), but also phylogenetic information (Mayr 2011). Thus, investigating the hindlimbs of pterosaurs may yield new phylogenetic and functional data. It is conceivable that the ankle joint includes diagnostic information that might be useful to characterize the approximately 200 nominal species known in Pterosauria. However, many specimens are incomplete and do not preserve this region of the skeleton, and when the hind limbs are preserved, in many cases the tarsal regions are enclosed in concretions (for example many, but not all, specimens from the Solnhofen limestones); others are badly crushed, have been displaced from their original position, or are simply lost. Among the approximately 70 specimens of ankle joints of pterosaurs preserved found in the literature (see Table 1), very few are sufficiently well-preserved to be compared with *P. guinazui*. For example, it can be noted that within the "non-pterodactyloid" pterosaurs, the tarsals of *Dorygnathus banthensis* (Padian 2008, SMNS 55886, SMNS 51827), *Campylognathoides liasicus* (Wellnhofer 1974, CM 11424; Padian 2008), *Eudimorphodon ranzii* (MCSNB 8950), *Peteinosaurus* (Dalla Vecchia 2003, MCSNB 3359, MCSNB 3496), four specimens of *Rhamphorhychus* (Wellnhofer 1975: fig. 17, 1978), and *Dimorphodon macronyx* (Padian 1983), are the only tarsals which can be compared to *P. guinazui* from the existing literature. In particular, the isolated tarsals of *Dimorphodon macronyx* (YPM 9182, YPM 350 M and R) have been preserved in three dimensions, and they were described by Padian (1983). Within the pterodactyloids, the tarsals of *Ctenochasma elegans* (described as *Pterodactylus elegans* in Wellnhofer 1970 [BSP 1875 XIV.501]), four specimens of the genus *Pterodactylus* (some of them are juveniles) (Wellnhofer 1970: fig. 8, 1978), *Anhanguera piscator* (Kellner and Tomida 2000, NSM-PV-19892), *Balaenognathus maeuseri* (Martill et al. 2023, NKMB P2011-633), *Tapejara* sp. (Kellner 2004, MN 6532-V), *Pteranodon* (unspecified species; Bennett 2001a, YPM 2462, KUVP 56650), and *Quetzalcoatlus northropi* (Padian 2017, TMM 42138-2, TMM 41954) can be compared to *P. guinazui* from published descriptions and illustrations. Bennett (1996) suggested that eight small specimens assigned to "*Pterodactylus*" *elegans* represented juveniles conspecific with the large specimens assigned to *Ctenochasma gracile*. Also, Bennett (2007) noted that the species associated with the epithet *elegans* has priority over *gracile* in the genus *Ctenochasma*, leading to the new combination *C. elegans*. Thus, the specimen referred to as *Pterodactylus elegans* Wagner, 1861 (Wellnhofer 1970: 48, pl. 8; Wellnhofer 1978: 25) now is the holotype of *Ctenochasma elegans* (BSP 1875 XIV.501). If most of the described tarsals mentioned above are trapped in the matrix and can only be described in one plane, some are preserved in three dimensions, as in *Anhanguera piscator*, *Tapejara* sp., both species of *Pteranodon*, and *Quetzalcoatlus northropi*.

Padian (2017) summarized, in a phylogenetic context, the morphology of the ankles of the pterodactyloids *Pterodactylus*, *Pteranodon*, *Tapejara*, and *Quetzalcoatlus*, and of other pterosaurs, such as *Dimorphodon*, *Dorygnathus*, *Campylognathoides*, *Rhamphorhynchus*. He has reported that in all these taxa, the distal tarsal bones have concave proximal facets that articulate with the medial and lateral condyles of the tibiotarsus. Distally, the distal tarsals articulate with metatarsals (MTs) II–IV, and the relatively large MT V articulates with the distolateral side of the lateral distal tarsal (Padian 2017).

In this work, although comparisons will be made with all pterosaur taxa that allow it, special attention will be paid to Pterodactyloidea. The morphology of the tarsals of pterodactyloids is better known in the more recent taxa than in the oldest ones, probably because of preservation bias, as we mentioned before. Indeed, rare are the representatives of

basal Pterodactyloidea that have detailed descriptions of the ankle joint in the literature (*Pterodactylus, Ctenochasma, Balaenognathus*). This is unfortunate because the appearance of the Pterodactyloidea constitutes a major event in the evolution of Pterosauria. The "non-pterodactyloid" pterosaurs are all small and can be considered as "good climbers and rare walkers" (Mazin and Pouech 2020: 39). Thus, all the mid-sized to giant pterosaurs belong to Pterodactyloidea, and they are considered to have been "good walkers". Even so, the locomotion of the "non-pterodactyloid" pterosaurs remains widely debated (Padian 2008; Witton 2015). A change in locomotor adaptations could have left a signature in the morphology of hindlimbs of pterosaurs, in particular the ankle joint. This is why studying basal pterodactyloids, such as the Ctenochasmatidae (Vidovic and Martill 2018; Andres 2021), may improve our understanding of the evolution of the ankle joint of Pterosauria and of its functional significance.

In this study, we detail the anatomy and structure of the ankle joint of numerous specimens of *Pterodaustro guinazui* Bonaparte, 1970, a ctenochasmatid pterosaur known solely from the lacustrine deposits of the Loma del *Pterodaustro* site from the Albian of Argentina (Chiappe et al. 1998). This filter-feeding pterosaur (Cerda and Codorniú 2023) is known from several specimens that represent various ontogenetic stages, from the embryo to an at least 3 m wingspan adult (Codorniú et al. 2017). Therefore, the detailed description of the ankle joint of *P. guinazui* increases the sample of pterosaur taxa for which the tarsus has been described and thus improves our understanding of the anatomy of basal Pterodactyloidea.

Institutional abbreviations.—BMNHC, Beijing Museum of Natural History, China; BNM, Bündner Naturmuseum, Chur, Switzerland; BPM, Beipiao Museum of Liaoning Province, China; BPMC, Beipiao Pterosaur Museum of China; BSP, Bayerische Staatssammlung für Paläontologie und Historische Geologie, Munich, Germany; CM, Carnegie Museum, Pittsburgh, USA; CYGB, Chaoyang Geological Park, Choyang, Liaoning Province, China; D, Dalian Natural History Museum, Liaoning Province, China; ELDM, Erlianhaote Dinosaur Museum, Inner Mongolia, China; ELTE, Eötvös University, Budapest, Hungary; FSA, Faculté des Sciences Aïn Chock, Casablanca, Morocco; GLGMV, Guilin Longshan Geological Museum, Guangxi Zhuan Autonomous region, China; GMN, Geological Museum of Nanjing, China; GMV, National Geological Museum of China, Beijing, China; GP/2E, Paleontologia Sistemática of the Instituto de Geociências at Universidade de São Paulo, Brazil; GPIT, Geologisch-Paläontologisches Institut, Tübingen, Germany; HIII, Henan Geological Museum, Zhengzhou, Henan Province, China; IGM, Universidad Nacional Autónoma de México (UNAM), Mexico City, Mexico; IVPP, Institute of Vertebrate Paleontology and Paleoanthropology (Chinese Academy of Sciences), Beijing, China; JME, Jura-Museum Eichstäitt, Germany; JPM, Jinzhou Museum of Paleontology, Liaoning Province, China; JZMP, Jinzhou Paleontological Museum, Liaoning Province, China; LPM, Liaoning Paleontological Museum, Shenyang Normal University, China; MB, Museum für Naturkunde Berlin, Germany; MCSNB, Museo Civico di Scienze Naturali, Bergamo, Italy; MFSN, Museo Friulano di Storia Naturale, Italy; MGUH, Geological Museum, University of Copenhagen, Denmark; MIC, Museo Interactivo de Ciencias, Universidad Nacional de San Luis, San Luis, Argentina; MIM, Mineral Museum of Beirut, Lebanon; MN, Museu Nacional, Departamento de Geologia e Paleontologia, Departamento Nacional da Produção, Rio de Janeiro, Brazil; MMP, Museo Municipal de Ciencias Naturales "Galileo Scaglia", Mar del Plata, Argentina; NKMB Naturkunde-Museum Bamberg, Germany; NMB, Naturhistorisches Museum Basel, Switzerland; NSM-PV Division of Vertebrate Paleontology, National Science Museum, Tokyo, Japan; PIN, Borissiak Paleontological Institute, Russian Academy of Sciences, Moscow, Russia; PVL, Instituto Miguel Lillo, Universidad Nacional de Tucumán, San Miguel de Tucumán, Argentina; SMNK, Staatliches Museum für Naturkunde Karlsruhe, Germany; SMNS, Staatliches Museum for Naturkunde Stuttgart, Germany; STM, Shangdong Tianyu Museum of Nature, Pingyi, Shandong Province, China; TMM, Texas Vertebrate Paleontology Collections, The University of Texas at Austin, Texas, USA; TMP, Royal Tyrrell Museum of Palaeontology, Drumheller, Alberta, Canada; UNCUYO-LD, Laboratorio y Museo de Dinosaurios, Universidad Nacional de Cuyo, Mendoza, Argentina; YPM, Peabody Museum of Natural History, Yale University, USA; ZIN PH, Paleoherpetological Collection, Zoological Institute of the Russian Academy of Sciences, Saint Petersburg, Russia; ZMNH, Zhejiang Museum of Natural History, Hanzhou, Zhejiang Province, China.

Other abbreviations.—LDT, lateral distal tarsal; MDT, medial distal tarsal; MT, metatarsal.

Material and methods

The preservation of *Pterodaustro guinazui* fossils is very peculiar; in most cases, they can only be observed in 2D, whereas 3D preservation is rare. Generally, the centers of the long or wide bones are crushed, while the joints are uncrushed. In all cases, they are trapped in the substrate and are too fragile to be removed. Therefore, there is only one view available for each fossil, but the preservation allows us to understand the three-dimensional structure of the fossils from the available views. The information presented in the description is based on all *P. guinazui* specimens known so far, as exposed. All cases of intraspecific variation are reported. The specimens included in the study, sorted by bone, are listed in Table 2.

The fossils were observed with a stereomicroscope Leica M-80, and the images taken with the associated Leica MC-190 HD whenever possible. Images of lesser degree of magnification were taken with an Olympus E-M10 Mark2.

Table 2. Studied specimens of *Pterodaustro guinazui*, sorted by ontogenetic stage.

Specimen	Bone or part of the skeleton represented	Ontogenetic stade	Justification of the attribution of the ontogenetic stage
MIC-V241	sub-complete specimen	early juvenile	Very small and has many unfused bones.
MMP 1168	tibiotarsus + foot	early juvenile	Very small and has many unfused bones.
MIC-V104	tibiotarsus + foot	late juvenile	Proximal tarsals unfused together and with the tibia.
PVL4549	tibiotarsus + foot	late juvenile	Proximal tarsals unfused together and with the tibia.
PVL3860	tibiotarsus + foot	late juvenile	Proximal tarsals unfused together and with the tibia.
MIC-V623	sub-complete specimen	sub-adult	Some unfused bones, particularly in the wrist and ankle, which is a sign of skeletal immaturity, but it is more mature than the juveniles, and some fusions appear to be in the process of being completed.
MIC-V243	sub-complete specimen	sub-adult	All its bone fusions completed, with only traces of a few sutures showing recent fusion remaining.
MIC-V627	tibiotarsus	sub-adult	Fusion of the tibiotarsus completed with a visible suture between former tibia and tarsals.
MIC-V28	tibiotarsus	sub-adult	Fusion of the tibiotarsus completed with a visible suture between former tibia and tarsals.
MIC-V85	tibiotarsus	sub-adult	Fusion of the tibiotarsus completed with a visible suture between former tibia and tarsals.
MIC-V169	tibiotarsus	sub-adult	Fusion of the tibiotarsus completed with a visible suture between former tibia and tarsals.
MIC-V379	tibiotarsus	sub-adult	Fusion of the tibiotarsus completed with a visible suture between former tibia and tarsals.
MIC-V120	tibiotarsus	sub-adult	Fusion of the tibiotarsus completed with a visible suture between former tibia and tarsals despite the distal end being partly cut off.
MIC-V80	tibiotarsus	sub-adult	Fusion of the tibiotarsus complete. There is a fracture of the fossil right between the tibia and the tarsals. They seems to have been fused, but the fact that the fracture occurred here may reflect a preliminary fragility at this point, and therefore a still fragile fusion. Added to the relatively small size of the fossil, we suggested that it was a sub-adult.
MIC-V3	tibiotarsus	adult	Completely fused tibiotarsus.
MIC-V157	tibiotarsus	adult	Completely fused tibiotarsus.
MIC-V90	tibiotarsus	adult	Completely fused tibiotarsus.
PVL3869	tibiotarsus	adult	Completely fused tibiotarsus.
MIC-V50	tibiotarsus	adult	Completely fused tibiotarsus.
MIC-V11	tibiotarsus	adult	Seems to have a completely fused tibiotarsus, but the state of the fossil makes it impossible to be sure. The tibiotarsus is long, which tends to confirm the previous obeservation.
MIC-V28	tibiotarsus	adult	Fusion of the tibiotarsus complete. The state of the fossil and its orientation doesn't admit the observation of eventual suture, but it size, one of the biggest of the tibiotarsus of *Pterodaustro guinazui*, allows us to suggest it is a remain of an adult.
PVL3970	tibiotarsus	?	The distal end is too damaged to conclude the ontogenetic stage of the specimen.
MIC-V629	metatarsal	?	Very small and gracile, should be between juvenile and sub-adult, but we have not observed a size-independent criteria related to skeletal maturity.
MIC-V93	metatarsal	?	Very small and gracile, should be between juvenile and sub-adult, but we have not observed a size-independent criteria related to skeletal maturity.
MIC-V103	metatarsals	?	We have not observed a size-independent criteria related to skeletal maturity.
MIC-V262	metatarsals	?	We have not observed a size-independent criteria related to skeletal maturity.
MIC-V105	metatarsals	?	We have not observed a size-independent criteria related to skeletal maturity. But the metatarsals are small, it could correspond to a sub-adult.
MIC-V248	metatarsals	?	The size is small, and it is maybe associated with 3 distal tarsals (before the fusion of the fusion of the distal tarsals II and III in MDT), but the preservation is not sufficient to be affirmative. It could correspond to a juvenile or a sub-adult.

Kellner (2015) noted that the term "subadult" was very imprecise, so he attempted to define ontogenetic stages (OS) in pterosaurs (based mostly on early pterosaurs) from OS1 to OS6. However, it is difficult to recognize these ontogenetic stages by looking at the ankles alone, as few of the characters that define Kellner's (2015) OS are found in the ankle. Therefore, although we appreciate Kellner's (2015) contribution, the partial and complete specimens of *P. guinazui* that we had at our disposal do not allow us to recognize the ontogenetic stages that he described. To de-

termine the relative age of the specimens (e.g., early or late juveniles, subadult, adult), we considered criteria that are not solely size-dependent that reflect skeletal maturity, as shown by the extent of ossification and fusion of the skeleton (Bennett 1993, 1995, 2018). As the majority of specimens described in this study are isolated tibiae or ankles, we observed the fusion of tarsal elements to determine their ontogenetic stage. Basically, if there is no fusion of the tarsals, the specimen is considered early juvenile or late juvenile. We modify slightly the ontogenetic nomenclature used by Bennett (2018), namely "small juvenile" and "large juvenile" to emphasize that these two stages differ not solely by size but also by the number of discrete elements and their degree of fusion, and to avoid mixing ontogenetic terms ("early" and "late") with the characters used to assess these stages, such as size. If there was a partial fusion of the tarsals, the specimen is considered sub-adult, and if there is complete fusion of the tarsals, the specimen is considered to be adult. For semi-complete fossils, the entire skeleton was observed. MIC-V241 is very small and has many unfused bones, so it is considered a hatchling (part of the "early juvenile" ontogenetic stage). MIC-V623 has some unfused bones, particularly in the wrist and ankle, which is a sign of skeletal immaturity, but it is more mature than the juveniles, and some fusions appear to have been in the process of being completed; it is thus considered sub-adult. MIC-V243 has all its bone fusions completed, with only traces of a few sutures showing recent fusion remaining (Codorniù et al. 2013), so it is considered a sub-adult, mature enough for some bone structures to be considered as representing the adult condition, but also young enough for the observable sutures to be discussed. A list of the examined specimens and their ontogenetic stage is found in Table 2.

Results

The ankle joint of pterosaurs is composed of two proximal tarsals, which may be fused to the tibia to form the medial and lateral condyles of the tibiotarsus, and two or three distal tarsals, depending on the species and ontogenetic stage.

As in many other pterosaurs, in some specimens of *Pterodaustro guinazui* that have not reached skeletal maturity, the astragalus and calcaneum clearly remain unfused with the tibia (Figs. 1, 2), and the distal facet of the tibia is flat (Codorniú and Chiappe 2004). In adult specimens that have reached skeletal maturity, the calcaneum and the astragalus are fused to the tibia, forming the two condyles of a tibiotarsus (Padian 1983; Bennett 2001a; David et al. 2022). In those cases, and in specimens of *P. guinazui* considered as small to medium-sized subadults, a suture can often be observed (Fig. 3; Codorniú et al. 2013). Depending on the degree of fusion, the suture may be visible (incomplete fusion, presenting a certain degree of immaturity) or not (complete fusion between the diaphysis of the tibia and the tarsals). In the most mature specimens,

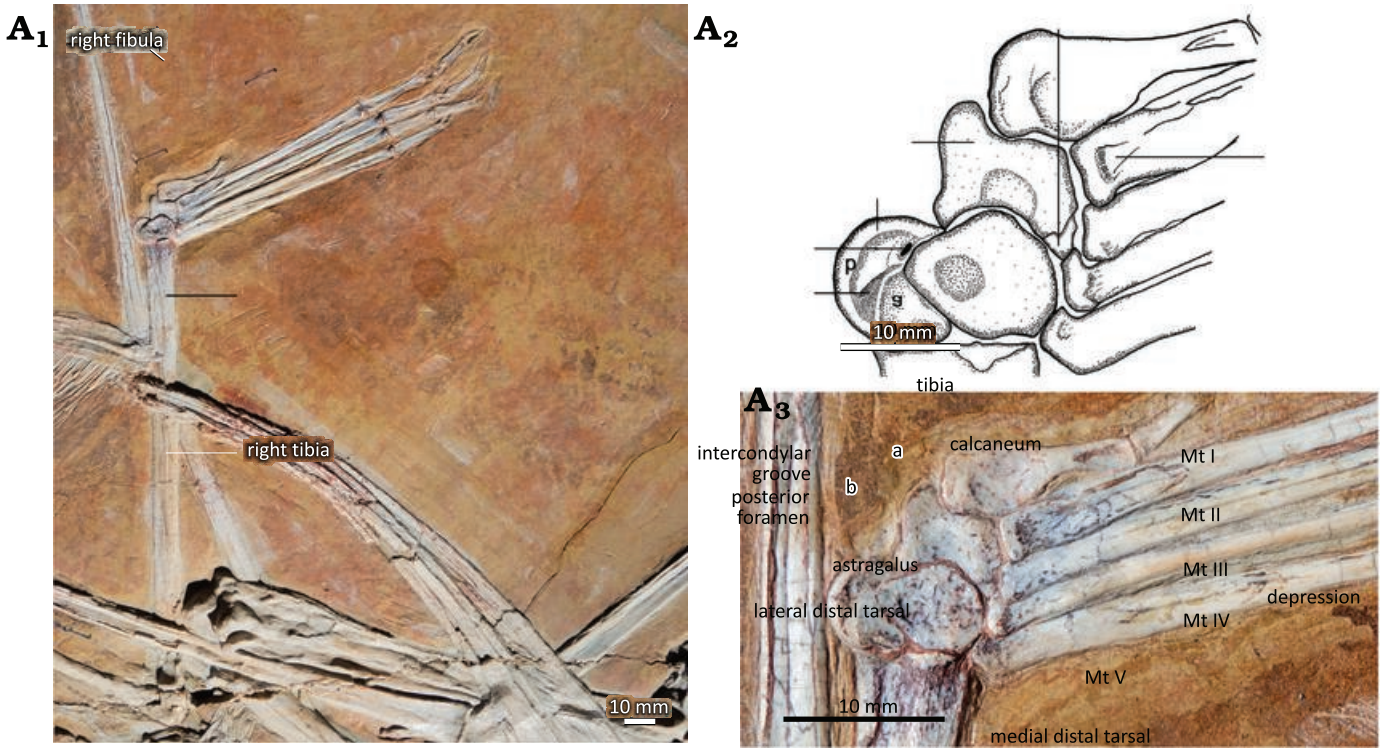

Fig. 1. Hindlimb of the ctenochasmatid pterosaur *Pterodaustro guinazui* Bonaparte, 1970, MIC-V623 (for the complete skeleton see Codorniú et al. 2013) from Loma del *Pterodaustro* site (Albian, Lower Cretaceous of Argentina). A_1, right tibia in postero-lateral view and foot in dorsal view; A_2, photograph of the ankle joint in lateral view (slightly postero-lateral); A_3, explanatory drawing of A_2. Abbreviations: Mt, metatarsal; for a and b see the text (pages 338–339).

Fig. 2. Unfused proximal tarsals of the ctenochasmatid pterosaur *Pterodaustro guinazui* Bonaparte, 1970, from Loma del *Pterodaustro* site (Albian, Lower Cretaceous of Argentina). **A**. MIC-V104; A_1, tibia in postero-lateral view and right foot in plantear view; A_2, details of proximal tarsals. **B**. MIC-V241; B_1, photograph of the complete skeleton of a juvenile; B_2, details of the two feet and tarsals. **C**. MMP 1168; C_1, right foot of a juvenile in plantar view; C_2, details of tarsals. Abbreviation: Mt, metatarsal.

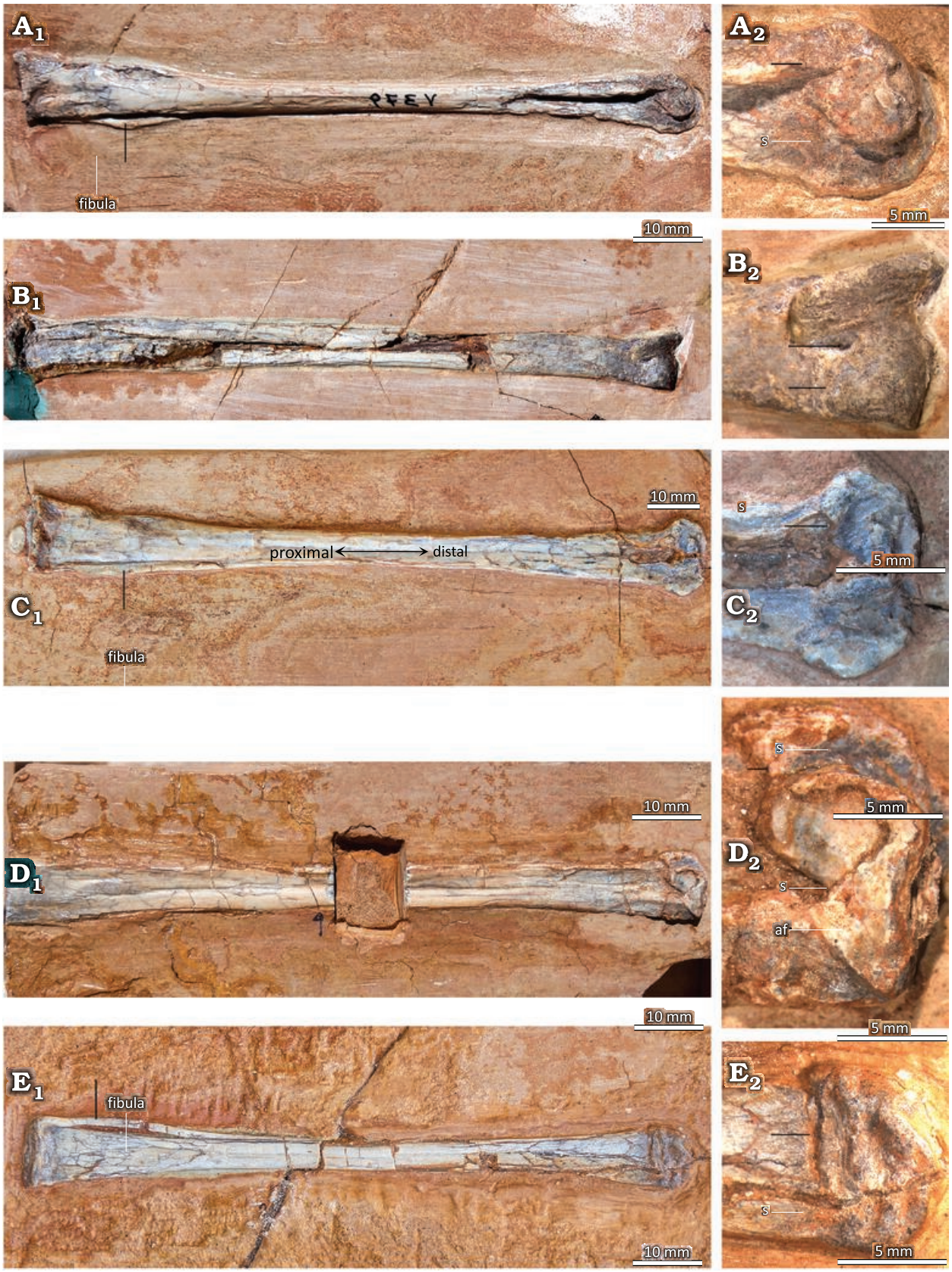

Fig. 3. Distal tibiotarsi of the ctenochasmatid pterosaur *Pterodaustro guinazui* Bonaparte, 1970, from Loma del *Pterodaustro* site (Albian, Lower Cretaceous of Argentina), with a visible suture. **A**. MIC-V627; A_1, anterior or posterior? view of complete tibiotarsus; A_2, distal end. **B**. MIC-V28; B_1, medial view of complete right tibiotarsus; B_2, distal end. **C**. MIC-V85; C_1, posterior? view of complete right tibiotarsus; C_2, distal end. **D**. MIC-V169; D_1, anterior view of complete right tibiotarsus; D_2, distal end. **E**. MIC-V379; E_1, medial view of complete right tibiotarsus; E_2, distal end. Abbreviations: af, anterior foramen; s, suture.

Fig. 4. Totally fused tibiotarsi of the ctenochasmatid pterosaur *Pterodaustro guinazui* Bonaparte, 1970, from Loma del *Pterodaustro* site (Albian, Lower Cretaceous of Argentina), without visible suture. **A**. MIC-V3; A_1, right foot in a latero-anterior view; A_2, distal end. **B**. MIC-V157; B_1, complete left? tibiotarsus in posterior? View; B_2, distal end. **C**. MIC-V90; C_1, complete left tibiotarsus in lateral view; C_2, distal end.

curiously only represented by partial or incomplete and isolated specimens in the *P. guinazui* sample, fusion is complete and sutures are no longer visible in the tibiotarsi (Fig. 4). It should be noted that MIC-V90 (Fig. 4C) shows a fracture which is the result of a taphonomic breakage, and is not a suture.

The lateral condyle of the tibiotarsus (Fig. 5: red) is elongated and oval in articular outline, and rounded in lateral view (Fig. 4C). In an anterior view (Figs. 3D, 5), it is extended proximally and distally, and slightly oblique to the shaft (more lateral in its distal part, and more medial in its proximal part). The articular facet (Fig. 5: red) for the

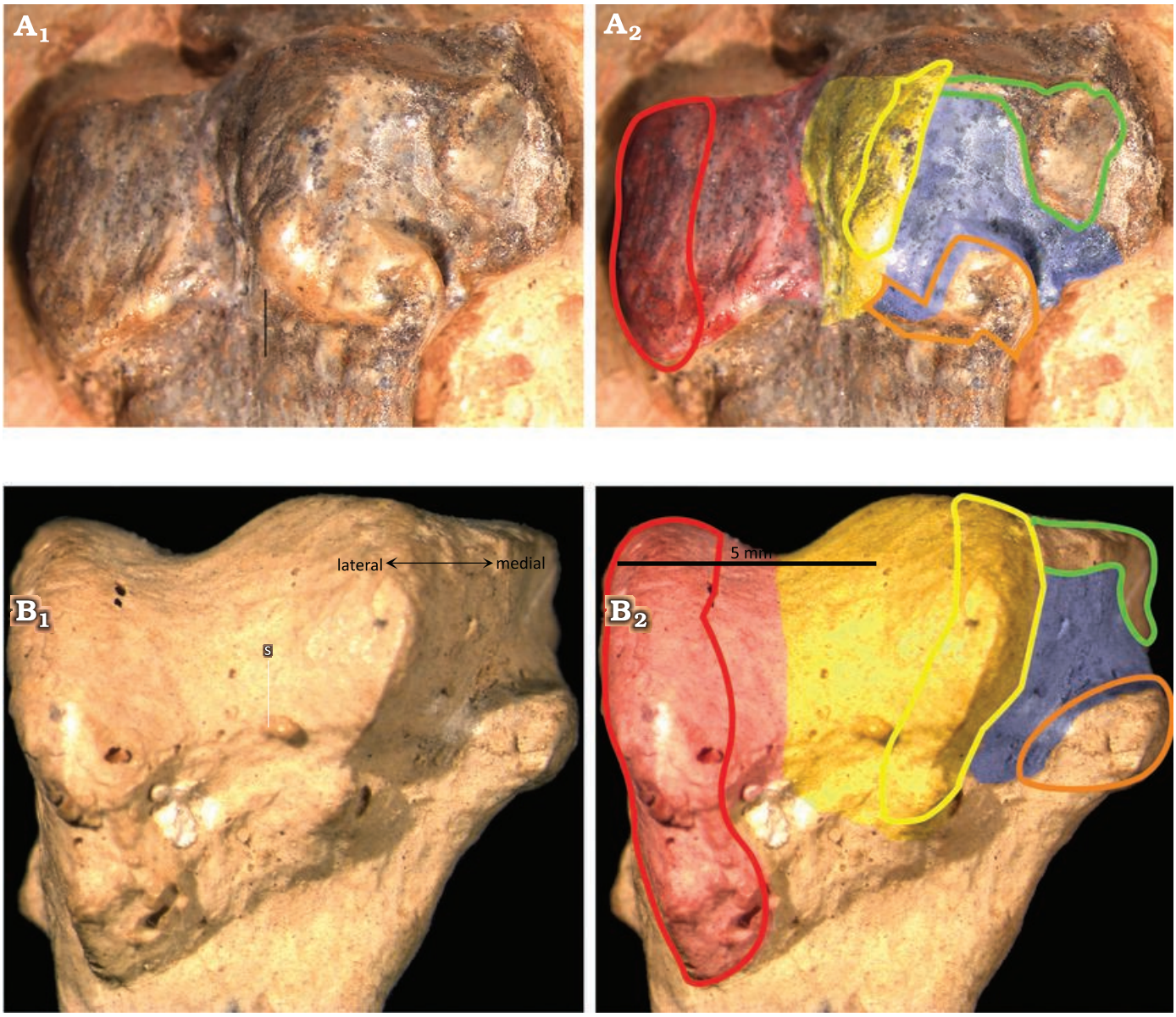

Fig. 5. The ctenochasmatid pterosaur *Pterodaustro guinazui* Bonaparte, 1970, from Loma del *Pterodaustro* site (Albian, Lower Cretaceous of Argentina), distal right tibiotarsus in posterior view. **A**. PVL3869; A_1, distal end; A_2, schematic drawing of the articular surfaces. **B**. MIC-V50; B_1, distal end; B_2, schematic drawing of the articular surfaces. Red shading, lateral condyle; yellow shading, medial condyle; blue shading, medial articular surface; red outline, articular prominence of the lateral condyle; yellow outline, articular prominence of the medial condyle; green outline, medio-distal ridge; orange outline, medio-distal prominence of the tibia forming the distal ridge of the medial articular facet. Abbreviation: s, suture.

lateral distal tarsal (LDT) allowed considerable rotation proximo-distally (Fig. 5). In anterior view, a foramen is visible between the two condyles (Fig. 3D). The medial condyle of the tibiotarsus (Fig. 5: yellow) is formed by the astragalus. It is less projected posteriorly and anteriorly than the lateral condyle, and barely projects distally. A third articular surface for the distal tarsals (Fig. 5: blue) can be observed in all mature specimens in which the medio-posterior part is visible (MIC-V28, V50, V85, V157, V243, V379, PVL3859; Figs. 3A, D, E, 4C, 5). A depression in this zone (Fig. 5: blue) is delimited by two small and pronounced ridges: a distal ridge (Fig. 5: green) on the astragalus, and another proximal ridge (Fig. 5: orange) on the tibia. Those ridges probably constrained rotation of the medial tarsal around the tibiotarsus; this new character will be discussed below.

In MIC-V623 (Fig. 1), the tibia is in lateral view (slightly postero-lateral), as suggested by the presence of the fibula on the proximal part of the tibia. The proximal tarsals are articulated in anatomical continuity with the tibia. Nothing suggests that they have been displaced post-mortem. The proximal tarsals are not yet fused to the tibia or to each other, but all three elements appear to be in the position where they subsequently fuse during ontogeny, as mentioned above. This shows the contribution of each bone to the tibiotarsus later in the ontogeny. Here we have interpreted the two bones articulated with the tibia as the two proximal tarsals. In keeping

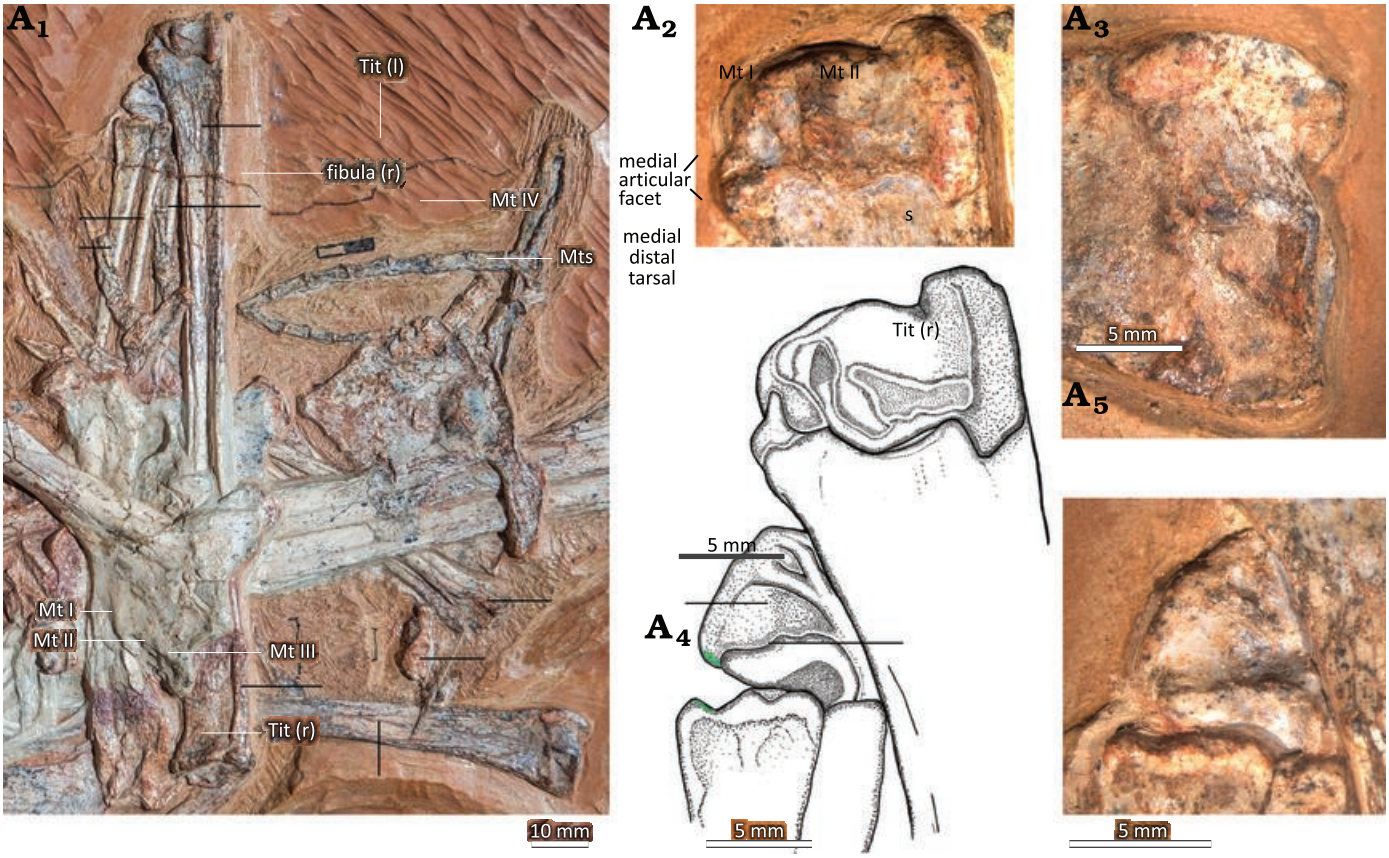

Fig. 6. **A**. Tibiotarsi of the ctenochasmatid pterosaur *Pterodaustro guinazui* Bonaparte, 1970, MIC-V623 (for the complete skeleton see Codorniú et al. 2013) from Loma del *Pterodaustro* site (Albian, Lower Cretaceous of Argentina). A_1, photograph of the two tibiotarsus; A_2, drawing of the right ankle joint; A_3, right medial distal tarsal; right (A_4) and left (A_5) distal tibiotarsus. Abbreviations: l, left; Mt, metatarsal; r, right; s, suture; Tit, tibiotarsus.

with classical amniote ankle structure, the more lateral of the proximal tarsals has been interpreted as the calcaneum, and the more medial of the proximal tarsals as the astragalus. In this specimen observable in lateral view (slightly postero-lateral), the astragalus is the most posterior bone of the ankle joint. It is composed of two parts. The first is a relatively rounded and thickened part (Fig. $1A_3$: a) that is the proximo-posterior continuity of the calcaneum in terms of volume and shape. Together with the calcaneum, this forms the lateral condyle of the future tibiotarsus. The second, medial part (Fig. $1A_3$: b) is crescentic in lateral view (slightly postero-lateral); it forms the medial condyle of the future tibiotarsus.

The calcaneum is pyriform in lateral view, oriented horizontally, with the narrow tip facing posteriorly (Fig. 1). There is a circular depression in the middle of the posterior half of the calcaneum, which could be a preservation artifact. The calcaneum articulates posteriorly with the astragalus (as mentioned above). There is a foramen between the astragalus and the calcaneum, very close to the narrow tip of the latter. Proximally the calcaneum articulates with the antero-lateral part of the distal tibia. The calcaneum of *P. guinazui* does not present a calcaneal tuber.

The distal tarsals are composed in Pterosauria of two or three elements (Padian 2017), depending on species and ontogenetic stage. When there are three elements, those distal tarsals are named distal tarsal II and III, and IV. When there are two elements, the distal tarsal IV is named lateral distal tarsal (LDT), and the fusion of the distal tarsals II and III is named medial distal tarsal (MDT).

In MIC-V243 (Fig. 6), the MDT is almost entirely visible and very well preserved; it is articulated with the metatarsal (MT) I and in contact with the MT II. The MDT is also observed in MIC-V623. The distal facet of the tarsal is comma-shaped in anterior view, with a small medial facet (Fig. 6: green zone). The MDT appears laterally offset from the metatarsals, but overall the shape of the part of the distal facet of the MDT that we can see mirrors the proximal facet of the metatarsal I. A suture can also be seen, located slightly proximal to the distal facet (Fig. 6), indicating that this tarsal is composed of two bones. It has been assumed in the literature that the MDT is a fusion of the distal tarsals II and III (Padian 2017). Here, it seems that we can observe this fusion, still marked by the suture. We exclude the possibility that one of the tarsals fusing here is the intermedium because of its: (i) shape, the intermedium appears to be a proximo-distally elongated bone in Ornithodira (Morse 1880); (ii) size, the bone is the largest of the tarsals we can observe in MIC-V243, in contrast to what has been described for the intermedium in *Pterodactylus* by Schaeffer (1941) and Romer and Parsons (1977); (iii) ontogeny, Piñeiro et al.

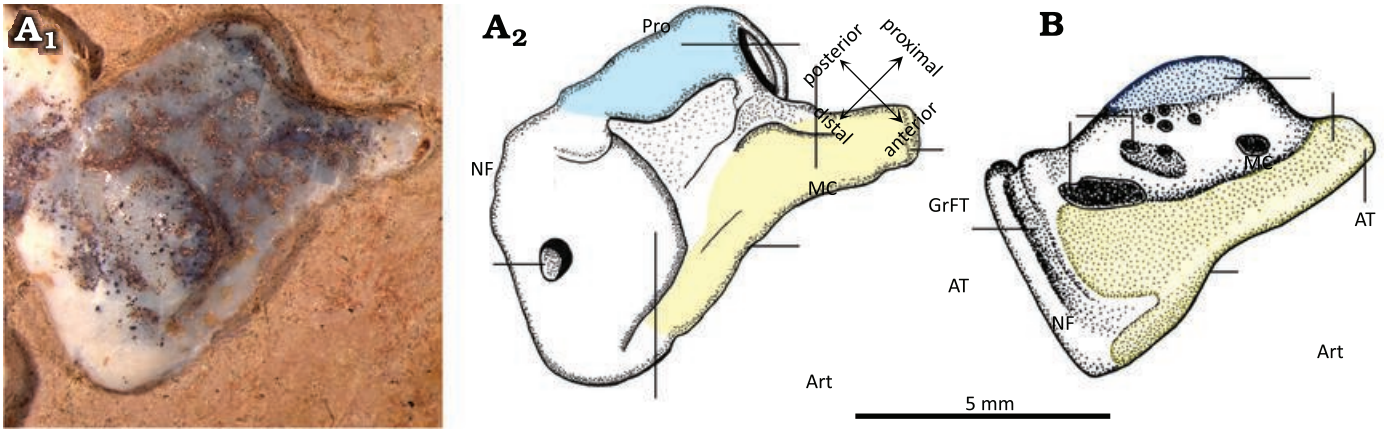

Fig. 7. Comparison of right medial distal tarsal (MDT) of the ctenochasmatid pterosaur *Pterodaustro guinazui* Bonaparte, 1970 (A) and the pteranodontid pterosaur *Pteranodon* (B). **A**. MIC-V104, from Loma del *Pterodaustro* site (Albian, Lower Cretaceous of Argentina); A_1, photograph of MDT in lateral view; A_2, drawing. **B**. YPM 2462, from USA (Campanian–Santonian) (drawing modified after Bennett 2001a). Yellow, proximal articular surface; blue, distal articular surface. Abbreviations: Art, articular surface; AT, anterior tubercule; GrFT, groove for flexor tendon; MC, insertion of the medial condyle; NF, nutrient foramen; Pro, processus.

(2016) suggested that the intermedium is incorporated into the astragalus during ontogeny and not into the distal tarsals.

In MIC-V104 (Fig. 7A), an isolated distal tarsal is exposed in lateral view; we interpret it as a right MDT because of its similarities to the MDT of *Pteranodon* described by Bennett (2001a; Fig. 7B). The MDT has a highly developed anterior tubercle. There is a well-developed posterior process. The proximal articular facet (Fig. 7: yellow) runs from the anterior tubercle to the process, and it does not extended far distally.

In MIC-V623 (Fig. 1), the foot (distal tarsals, MTs, and digits) has shifted slightly from its original position. The MDT, LDT, MTs and digits are visible in dorsal view. We interpret the most lateral distal tarsal, articulating with MTs V, IV, and III, as the LDT. Thus, we interpret the bone hidden behind the forming tibiotarsus, in contact with the MTs and medial to the LDT, as the MDT. In proximal view, the LDT is sub-rectangular, with three concave sides (only the side in articulation with the metatarsals IV and III is nearly straight). It is waisted, with slightly extended posterior corners. The antero-medial corner of the proximal face of the LDT of that specimen shows a narrow contact with the MDT, which is hidden by the surrounding elements. As the MDT is preserved under the tibiotarsus, only a small part of the articulation between the distal tarsals can be described. The concave proximal facet probably articulated with the lateral condyle (calcaneum) of the tibiotarsus, as suggested by its position and the fact that it fits with the roundness of the lateral condyle of the tibiotarsus. Dalla-Vecchia (2009) proposed a similar interpretation for *Carniadactylus rosenfeldi*. Distally, the LDT articulates with the MT IV, partially with the MT III, and laterally with the MT V. Padian (2017) proposed that the LDT is homologous with the distal tarsal IV. This is compatible with our observations, because the embryo (Codorniú et al. 2018) and MMP 1168 (Fig. 2C) have only three preserved distal tarsals. The shafts of the metatarsals (MTs) of *P. guinazui* are straight, with the proximal ends slightly wider than the distal ends (Fig. 8). In MIC-V623 (Figs. 1, 8B) metatarsals (MTs) are exposed in a dorsal view; the proximal ends of the MTs I to IV are probably not in their original anatomical position relative to the tibiotarsus. As mentioned above, skeletal crushing seems to have slightly rotated the feet (which explains why the proximal part of the LDT is exposed, as mentioned above), and also makes the most medial MTs seem to be in contact with the proximal tarsals (or even with the tibia for the MT I). In anatomical position, these bones would have articulated with the LDT and the distal tarsal positioned medial to the LDT that is preserved beneath the tibiotarsus, which we interpret here as a MDT. Indeed, in MIC-V243 (Fig. 6), MT I is articulated with the MDT. However, in MIC-V623 (Fig. 8B), it appears that the MTs are still in anatomical position relative to each other. In their proximal part, the MTs I to IV overlap, with the lateral part of the MT I partially plantar to the MT II, etc.

The proximal ends of the MTs I to IV are distinctly subtriangular (Fig. 9) and show a concave proximal surface that articulated with the distal tarsals. The fossae are difficult to interpret in *P. guinazui*, due to the state of preservation. Indeed, many of the fossil shafts have been crushed and the center of the shafts has collapsed. However, it appears that a small triangular depression, exposed in dorsal view (Fig. 9), is not due to a taphonomic artifact. The length of this depression is about 5 mm from the proximal end of the MTs I to IV and does not vary with the length of the MT, at least in adults (observed in specimens with MT to 5–8 cm). The function of these depressions is probably for insertions of the M. tibialis anterior and other flexor muscles of the ankle, as suggested by Bennett (2001a) for *Pteranodon*. In plantar view, there is a depression less marked than in the dorsal one. From this plantar depression, the MTs present a long narrow scar on their plantar surface that reaches the distal depression of the posterior part of the MTs (see below).

Between the MTs I to IV of the specimen MIC-V623, the sediment is light greenish gray (Fig. 10) rather than the

Fig. 8. Metatarsals I–IV of the ctenochasmatid pterosaur *Pterodaustro guinazui* Bonaparte, 1970, from Loma del *Pterodaustro* site (Albian, Lower Cretaceous of Argentina). **A**. MIC-V104, right metatarsals in plantar view. **B**. MIC-V623, right foot in dorsal view. **C**. MIC-V103, dorsal view. **D**. MIC-V248, two feet in dorsal view. **E**. MIC-V262, two feet in plantear view. **F**. MIC-V105, two feet in plantar view. Abbreviation: PG, plantar groove.

reddish-orange color of almost all the rest of the skeleton (e.g., Fig. 1 on the contours of all the tarsals). The other places where sediment of this nature has been identified in *P. guinazui* is in the stomach contents in this same specimen (Codorniú et al. 2013), in the endocranium of many skulls (Codorniú et al. 2016), and inside the egg (Chiappe et al. 2004; Codorniú et al. 2018). In each case, they have been associated with remains of degraded soft tissues, and the light greenish gray color (Mussel scale: 5GY 8/1) is explained as the result of post-sedimentary chemistry (reduction stain). This specimen shows that soft tissues were probably present between the metatarsal I to IV, for at least half of their length. We cannot precisely determine the breadth or length of this possible structure. This could correspond to skin, muscles, nerves, blood vessels and, probably, a combination of these.

The distal ends of the MTs are straight to slightly convex (Fig. 11); they widen slightly, but less than the proximal ends of the MTs. In plantar view (Fig. 11B), a depression in this widening probably shows the location of muscles or insertion of the extensor tendon. A groove is visible all along

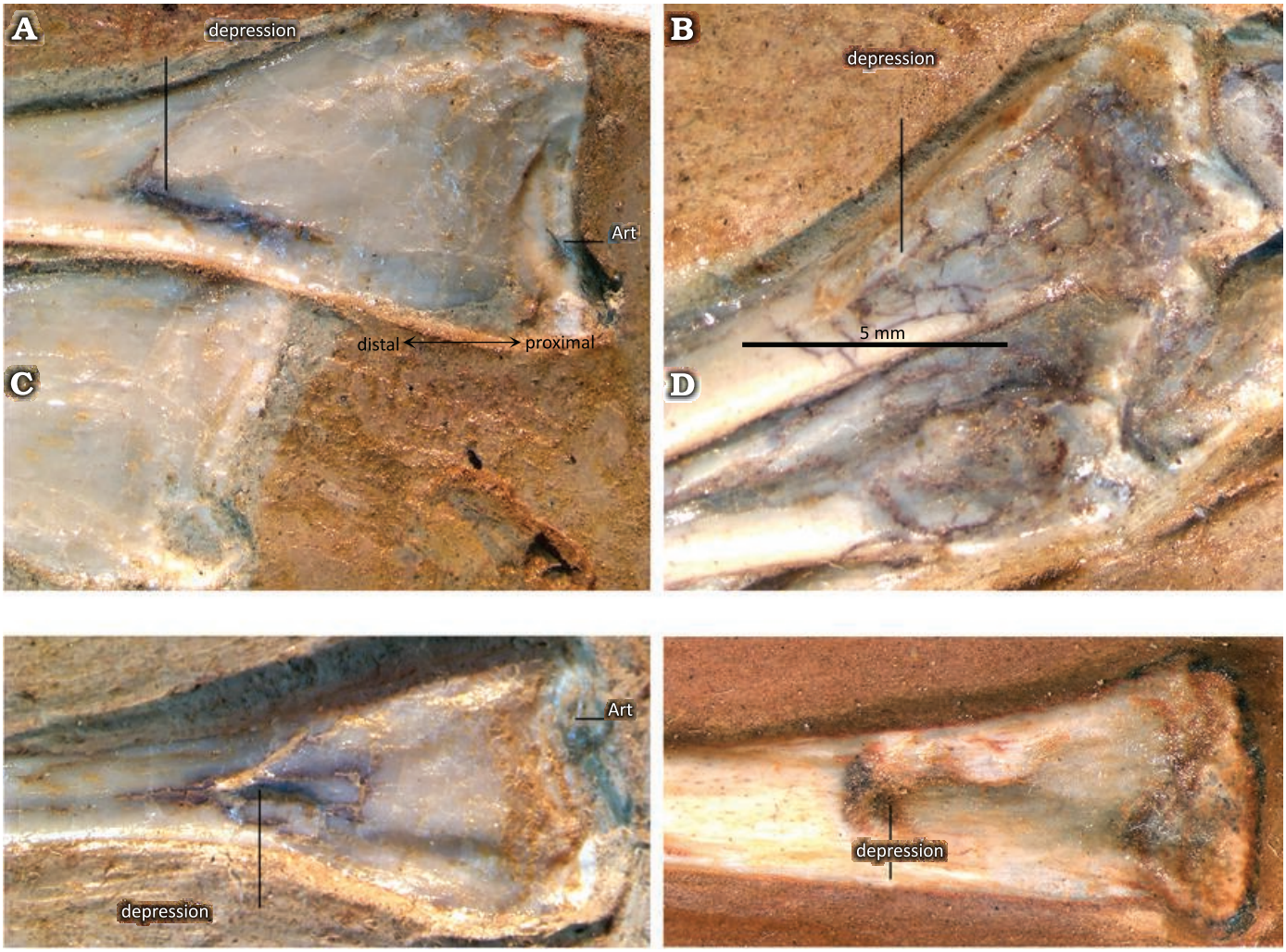

Fig. 9. Proximal metatarsals (in an anterior view) of the ctenochasmatid pterosaur *Pterodaustro guinazui* Bonaparte, 1970, from Loma del *Pterodaustro* site (Albian, Lower Cretaceous of Argentina). **A**. MIC-V93. **B**. MIC-V629. **C**. MIC-V103. **D**. MIC-V248. Abbreviation: Art, articular surface.

Fig. 10. Right ankle joint of the ctenochasmatid pterosaur *Pterodaustro guinazui* Bonaparte, 1970, MIC-V623, from Loma del *Pterodaustro* site (Albian, Lower Cretaceous of Argentina), the tibia and proximal tarsals in lateral view, the foot is slightly displaced, so lateral distal tarsal and metatarsals are in dorsal view; A_1, photograph of the complete foot; A_2, detail of the metatarsal zone. Abbreviation: IM, interdigital membrane.

the plantar part of the MTs (Fig. 8A, F), from the proximal end, along the shaft of the MTs, to the distal, widened end; this may mark the insertion of a tendon connecting the distal MTs to the distal tarsals. These grooves may also result from a preservation artifact due to the collapse of some shafts, as mentioned above. Thus, more specimens are needed to assess the significance of this groove.

The hooked MT V (Fig. 12) is articulated with the lateral part of the LDT; it measures about quarter of the length of the other MTs. Its proximal part is wider than the other MTs, it

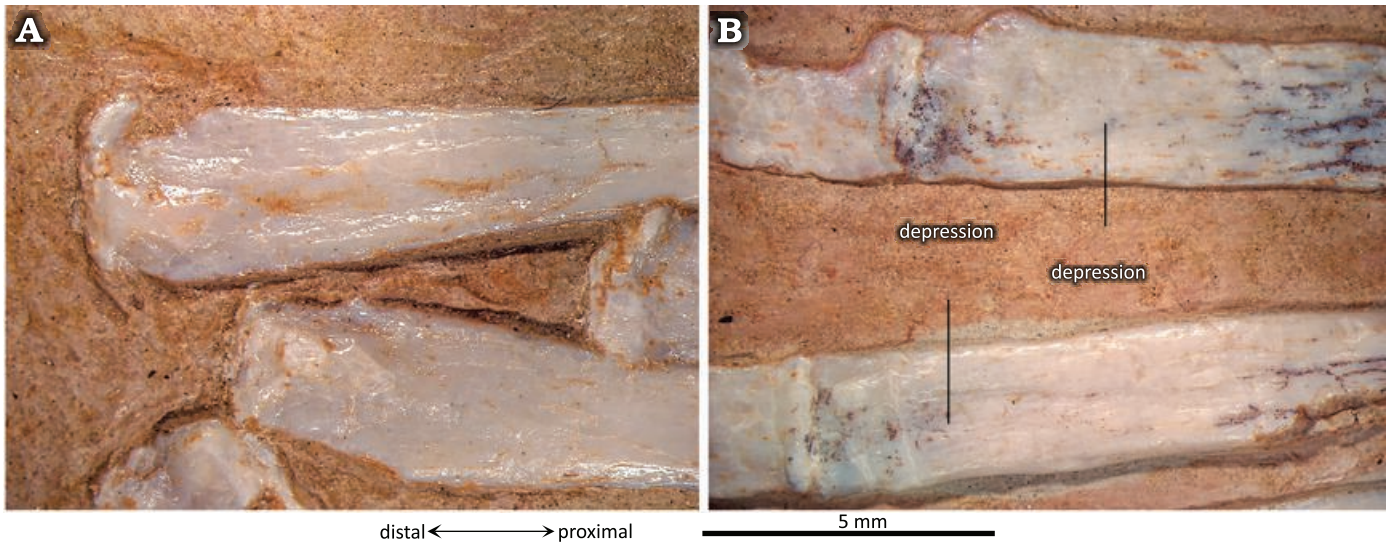

Fig. 11. Distal end of metatarsals of the ctenochasmatid pterosaur *Pterodaustro guinazui* Bonaparte, 1970, from Loma del *Pterodaustro* site (Albian, Lower Cretaceous of Argentina). **A**. MIC-V103 in dorsal view. **B**. MIC-V104 in plantar view.

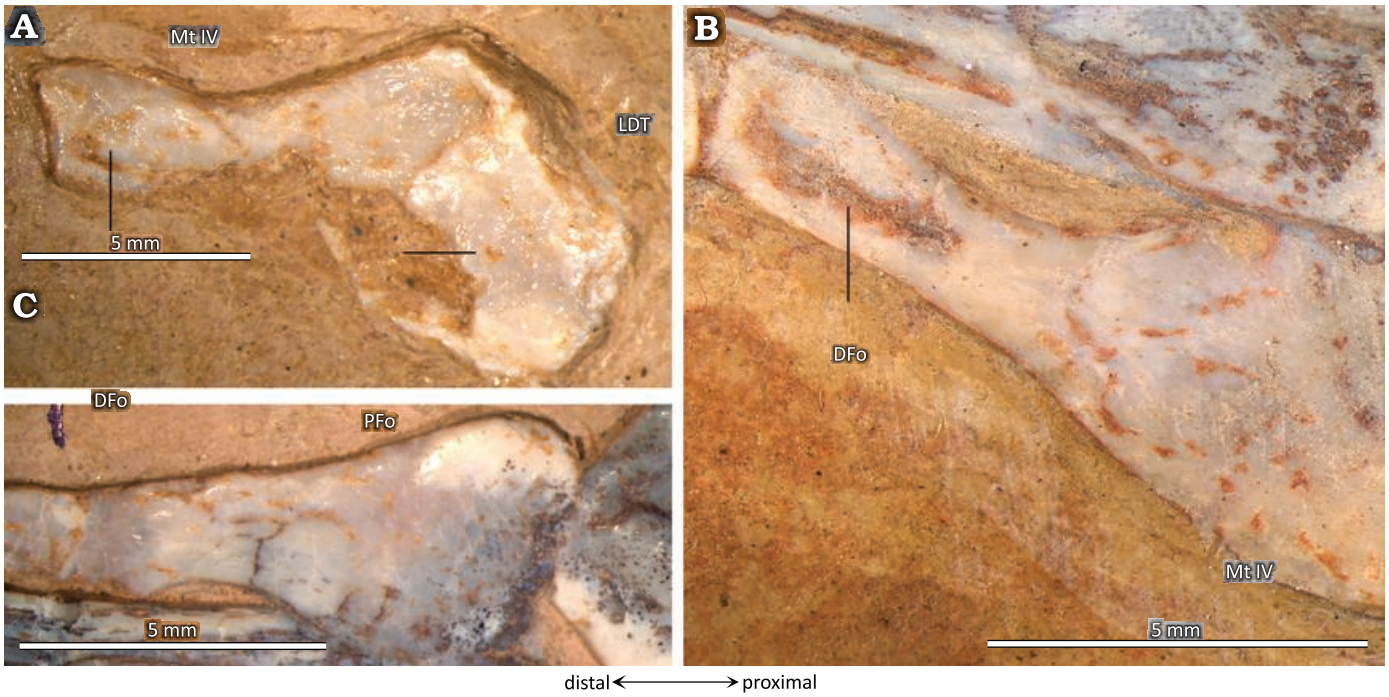

Fig. 12. Metatarsal V of the ctenochasmatid pterosaur *Pterodaustro guinazui* Bonaparte, 1970, from Loma del *Pterodaustro* site (Albian, Lower Cretaceous of Argentina). **A**. MIC-V104 in posterior view. **B**. MIC-V623 in anterior view. **C**. MIC-V103 in anterior view. Abbreviations: DFo, distal fossa; LDT, lateral distal tarsal; Mt, metatarsal; PFo, proximal fossa.

displays a fossa (PFo), and it may have been the site for tendinous attachments of muscles. If so, the position of this fossa suggests that the muscles that attached here were involved in foot flexion. In its distal part, there is another fossa (DFo).

In general, fewer foramina can be observed in the hindlimb of *P. guinazui* than in other well-preserved pterosaurs (Bennett 2001a). The only foramina that can be observed are large: two between the medial and lateral condyles of the tibiotarsus (in anterior and posterior part; Figs. 1, 3D), and another in the lateral view of the MDT (Fig. 7). It seems that this may be due to a preservation artifact that smoothed out the surfaces of the bones, thus hiding the smaller foramina. Future studies, using non-invasive technologies to observe the internal structure of these bones, could shed further light on this issue.

Discussion

Generally in Pterosauria, the proximal tarsals (astragalus and calcaneum) are fused to the distal end of the tibia, which hampers inter-specific comparisons based on speci-

mens of different degrees of skeletal maturity. Thus, in the "non-pterodactyloid" pterosaurs, the distal end of the tibia seems to be flat (Wellnhofer 1975, 1978; Dalla Vecchia 2003; Padian 2008), possibly associated with a skeletal immaturity and eventual unpreserved cartilaginous tissues. This condition, also observed in *Pterodaustro guinazui* (Figs. 1, 2), in the Ctenochasmatidae *Balaenognathus maeuseri* (Martill et al. 2023, NKMB P2011-633) and in the azhdarchid *Cryodrakon boreas* (Currie and Jackobsen 1995), seems to be the general condition for Pterosauria. Surprisingly, in two almost complete skeletons of *P. guinazui* that present clear differences in wingspan (e.g., MIC-V243: 1.60 m and MIC-V623: 2 m), the smaller specimen (MIC-V243) shows more fusion of some bones and in the tibiotarsi than in the larger (MIC-V623) specimen. This may reflect sexual dimorphism or intraspecific variability, a common phenomenon previously documented in developmental studies (Olori 2013; Laurin et al. 2022). The significance of this observation will be assessed in future studies, based on an analysis of all the evidence for fusion in the extensive growth sequence of *P. guinazui*.

It seems that fusion of the tibia with the proximal tarsals occurs after fusion between the proximal tarsals. Indeed, in the "non-pterodactyloid" pterosaur *Anurognathus ammoni* (Bennett 2007, SMNS 81928) and the pterodactyloid *Zhenyuanopterus longirostris* (Lü 2010, GLGMV 0001), the tarsals are fused to each other but not with the tibia. In *P. guinazui*, we can observe three conditions: (i) in the youngest specimens the tarsals are not fused, they are present as small, discrete bones (Fig. 2); (ii) in the subadults the tibiotarsus is formed, but with the suture between the tibia and tarsals still visible (Fig. 3); (iii) in the adults, the tibiotarsus is entirely formed, without any suture between the fused elements (Fig. 4). In the observed specimens of *P. guinazui*, when the proximal tarsals are fused to each other, they are fused with the tibia too. In specimens where the tibia and the proximal tarsals are fused but the suture is still visible (i.e., ontogenetically recent fusion is assumed) (Fig. 3), sutures between the calcaneum and the astragalus cannot be distinguished. Therefore this seems to indicate that tarsal fusion precedes tibiotarsal fusion in *P. guinazui* too. But both fusions seem to happen in close succession, which would explain the absence of specimens with fused proximal tarsals unfused with the tibia in *P. guinazui*, and the rarity of this hypothesized ontogenetic condition in the pterosaur fossil record, given that only 3% of ankle specimens found in the literature (Table 1) show fused proximal tarsals but no fusion between the proximal tarsals and the tibia. However, it is difficult to directly correlate the occurrence of these fusions with differences in ontogenetic age. Indeed, previous studies have already shown that the various ontogenetic events cannot be related in a linear relationship, either to time or to body size (Laurin and Germain 2011).

In *P. guinazui*, the best-preserved specimen (MIC-V623) of unfused proximal tarsals is conserved in a condition that only exposes them in lateral view (slightly postero-lateral), as shown in the description (above). Although some pterosaur specimens include isolated elements preserved in three dimensions, the description of the proximal tarsals in lateral view is not always available, for example *Peteinosaurus* and *Eudimorphodon* (Dalla Vecchia 2003) or *Tapejara* (Kellner 2004), which complicates comparisons between *P. guinazui* and other taxa. Only the isolated tarsals of *Anhanguera piscator* have been described in lateral view in the literature (Kellner and Tomida 2000). The calcaneum of *A. piscator* is the smallest of the proximal tarsals, and has no calcaneal tuber, as in *P. guinazui*. In *P. guinazui*, MIC-V623 shows that the lateral condyle of the tibiotarsus is not only composed of the calcaneum (Fig. 1). In lateral view, the pyriform calcaneum has a pointed posterior apex, but the posterior part of the lateral condyle is rounded, because part of the astragalus (a in Fig. $1A_3$), completes the condyle. Therefore, the complete lateral condyle of the tibiotarsus is formed by the calcaneum and a part of the astragalus. A similar condition has been described in *A. piscator* by Kellner and Tomida (2000). Also, the observations made in the posterior part of the proximal tarsals of MIC-V623 suggest that the intercondylar groove and the medial condyle of the tibiotarsus are only composed of the astragalus. Kellner and Tomida (2000) observed that there is no intercondylar groove in the posterior part of the proximal tarsus complex in *A. piscator*, contrary to what can be observed in *P. guinazui* (Fig. 1: IG).

In *P. guinazui*, the lateral condyle is more rounded and extends further distally than the medial one, and it is thus slightly longer, as in *Peteinosaurus*, *Eudimorphodon*, and *Dimorphodon* (Dalla Vecchia 2003; Padian 1983). It differs from the tibiotarsus condyles of *Pteranodon*, whose condyles are subequal in shape and size (Bennett 2001a), and from *Azhdarcho lancicollis*, whose tibiotarsus is similar to that of *Pteranodon*, except that the articular surface of the condyles extends more proximally on the posterior side in *Pteranodon* (Averianov 2010).

In *P. guinazui,* the well-developed medial surface of the tibiotarsus (Fig. 5: blue shading) articulates with the MDT. As the medial condyle of the tibiotarsus of *P. guinazui* (delimited by a yellow line in Fig. 5) barely extends distally, this medial surface (Fig. 5: blue shading) is clearly for the articulation with the MDT. This forms a third concave articular surface, delimited proximo-distally by two ridges: one formed by the tibia (Fig. 5: orange outline) and the other by the astragalus (Fig. 5: green outline). Thus, the MDT, in its anatomical position, is blocked proximally and distally by these two ridges (Fig. 5: orange and green outlines). This condition is currently not documented in other Pterosauria in the literature. This structure seems to allow little amplitude for the flexion-extension movement of the foot, at least for the medial part of the foot. Indeed, even though the articulation of the MDT seems to be restricted between the two posterior ridges of this medial part of the tibiotarsus, the very rounded lateral condyle (in lateral view) allowed a great amplitude in antero-posterior rotation with the LDT. This observation suggests that there was an asymmetry of

the articulation of the foot, with a great lateral amplitude of flexion-extension movement, and a smaller medial amplitude of flexion-extension movement. If the movement of the two distal tarsals (LDT and MDT) was parallel to the axis of the tibiotarsus, the fact that the movement of the MDT is much more restricted than that of the LDT means that during extreme flexion and extension movements, the two distal tarsals would no longer be in contact (if the two distal tarsals are not fused). On the contrary, if the movement of the two distal tarsals was slightly diagonal to the axis of the tibiotarsus, during extreme flexion and extension movements, the two distal tarsals would remain in contact. The lateral condyle is oriented obliquely, such that its extremities are equidistant from the most medial zone of the joint. This orientation suggests that the distal tarsals remain in contact during joint movement. The complete relation between the MDT and LDT cannot be observed, so it is not possible to determine the nature of this articulation. As far as we know, the distal tarsals are articulated and unfused in Pterosauria (Dalla Vecchia 2003; Kellner 2004). They function as independent structures even in the stages that have reached skeletal maturity. As a result, our interpretation of an asymmetrical meso-tarsal articulation cannot be excluded. This kind of movement could correspond to the type of movement observed in the feet of the swimming birds (Clifton and Biewener 2018). If some Ctenochasmatidae waded as previously proposed for *Baleanognatus mauseri* (Martill et al. 2023), this would support this hypothesis. However, more studies are necessary to better understand the movement of this articulation, and obtaining CT scans in future studies would be useful to understand this peculiar articulation. Zeffer and Norberg (2003) proposed a diagram to discriminate the ankle of wading birds from the ankle of other birds, but the ankle structure of the birds differs sharply from that of pterosaurs because there is a tarsometatarsus in birds. Finally, in the most juvenile specimens of *P. guinazui* (Fig. 2B, C), the tibia does not seem to be part of the articulation with the distal tarsals, contrary to what is observed in adults and sub-adults. This structure may form shortly before adulthood or be correlated to the body size of the animal.

As mentioned in the description (above), the distal tarsals are composed in Pterosauria of two or three elements (Padian 2017): the distal tarsal IV, named LDT, and the distal tarsals II and III, which can fuse into a MDT. The LDT of the early pterosaur *Peteinosaurus* (Fig. 13A) described by Dalla Vecchia (2003) is preserved in a proximal view. In the specimen MIC-V623 (Fig. 1), we interpret the exposed surface of the LDT as the proximal face because it features a concave facet that may have articulated with the lateral condyle of the tibiotarsus. Thus, in a proximal view, the two bones are similarly waisted, but the LDT of *Peteinosaurus* is thinner and more constricted in its center (Fig. 13A).

The lateral and medial sides of the LDT of the "non-pterodactyloid" pterosaur *Dimorphodon* (Fig. 13B) are concave, but not the anterior and posterior sides, which are more flat (Padian 1983); the element is thus waisted. In proximal view,

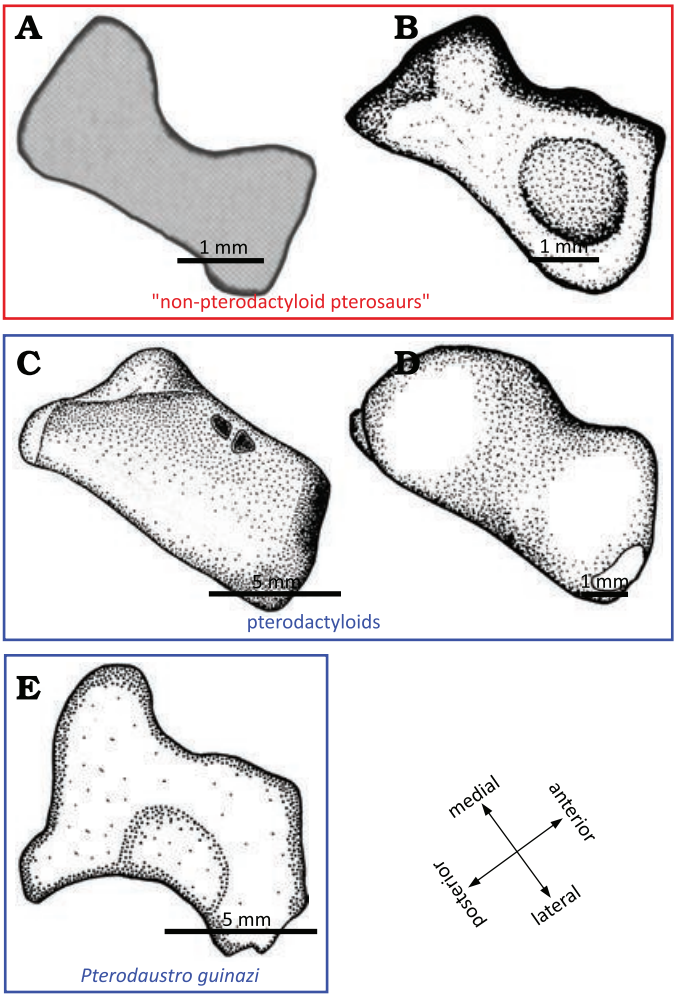

Fig. 13. Lateral distal tarsals. **A**. *Peteinosaurus*? *ranzii* (Zambelli, 1973) MCSNB-3359, from Zorzino Limestone Formation, Alaunian (modified after Dalla Vecchia 2003). **B**. *Dimorphodon macronyx* Buckland, 1829, YPM-350, from Blue Lias Formation, Hettangian (modified after Padian 1983). **C**. *Pteranodon*, YPM 2462, from USA, Santonien–Campanien (modified after Bennett 2001). **D**. *Tapejara* sp. MN6532-V, from Romualdo Formation, Aptian (modified after Kellner 2004). **E**. *Pterodaustro guinazui* Bonaparte, 1970, MIC-V623, from Loma del *Pterodaustro* site (Albian, Lower Cretaceous of Argentina).

the LDT of *Dimorphodon* is more trapezoidal than rectangular, with the lateral side shorter than the medial. The concave articular surface for the tibiotarsus of *Dimorphodon macronyx* is in the anterior part of the proximal facet of the LDT and it is very rounded; in *P. guinazui,* this concavity covers all of the proximal facet of the tarsal, which is thus not rounded.

In the late pterodactyloid *Pteranodon* (Fig. 13C), the proximal surface of the LDT appears to be slightly concave (Bennett 2001a), as in *P. guinazui.* But the LDT of *Pteranodon* differs in its trapezoidal shape, with relatively straight sides, whereas in *P. guinazui* it is waisted, with the slightly extended posterior corners. The LDT of the late pterodactyloid *Tapejara* (Fig. 13D) is similar to the LDT of *Pteranodon,* but with concave lateral sides and with convex anterior and posterior sides, in proximal view.

The LDT of *P. guinazui* is more robust than the LDT of *Dimorphodon macronyx* and *Peteinosaurus zambellii*, which seems to be thinner medio-laterally. But the LDT of *P. guinazui* shares with the two other taxa its waisted shape, which does not occur in *Tapejara* or *Pteranodon* (Fig. 13). This increasing robustness of the LDT, the largest of the distal tarsals, could be linked to "good walking" locomotion (Mazin and Pouech 2020) and may increase ability to bear weight on the ankle, and it may thus be one of the elements that enabled pterodactyloids to become heavier. However, study of a larger sample of early and late pterodactyloids is required to test these hypotheses.

Padian (2017) suggested that the MDT is a fusion of the distal tarsals II and III. Several pterosaur specimens display three distal tarsals, because they retain separate distal tarsals II and III. In "non-pterodactyloid" pterosaurs, the occurrence of three distal tarsals is relatively frequent; it occurs in *Rhamphorhychus muensteri* (Wellnhofer 1975), *Eudimorphodon ranzii* (Dalla-Vecchia 2003), *Changchengopterus pani* (Lü 2009), among others (Table 1). The intermedium is a possible third tarsal, as suggested by Schaeffer (1941) in *Pterodactylus* (Wellnhofer 1991: 57, unspecified species and specimen number), an interpretation shared by Romer and Parsons (1977). But Padian (2017) remarked that this bone (the intermedium) is not known in other pterosaurs or Ornithodira; thus, he interprets this bone as a tarsal that fused in more mature individuals, namely, the distal tarsal III.

In the late pterodactyloids, the fossil record does not document unfused distal tarsals II and III. Even in the *Anhanguera piscator* specimen described by Kellner and Tomida (2000), or the *Sinopterus dongi* described by Shen et al. (2021), which retain discrete calcaneum and astragalus and thus appear fairly immature, there are only two distal tarsals. The embryo of *P. guinazui* (Codorniú et al. 2017, MIC-V246) and the juvenile MMP 1168 (Fig. 2C) show three distal tarsals. In the sub-adult specimen of *P. guinazui* MIC-V243 (Fig. 6), a suture is visible between distal tarsals II and III (MDT). And in adults, only two elements (LDT and MDT) remain. The only four species of pterodactyloids that document unfused distal tarsals II and III are *Pterodactylus* (Wellnhofer 1991: 57, unspecified species and specimen number), *Balaenognathus maeuseri* (Martill et al. 2023), *Ctenochasma elegans* (Wellnhofer 1970; Bennett 2007) and *P. guinazui*, all placed phylogenetically as basal pterodactyloids (Vidovic and Martill 2018; Andres 2021). The paucity of hatchling occurrences in the fossil record of late pterodactyloids may partly explain why no specimens with three distal tarsals are known; the number of distal tarsals in late pterodactyloid hatchlings remains unknown. The number of pterosaur ankles preserved is similar in "non-pterodactyloid" pterosaurs and pterodactyloids (around 35 specimens in each group, see Table 1). The fact that the former regularly preserve three tarsals, while the latter do not, excepting in some basal pterodactyloids, suggests that these bones fused earlier in the geologically most recent pterosaurs.

An isolated distal tarsal, MIC-V104 (Fig. 7), had been interpreted as a MDT in a lateral view for its similarities with the MDT of *Pteranodon* described by Bennett (2001a). The MDT of MIC-V104 has a larger anterior tubercle than in *Pteranodon*. The proximal articular surface (Fig. 7: yellow) is less extended than in *Pteranodon*. The posterior part of the MDT of *P. guinazui* presents a large process, whereas *Pteranodon* shows a groove for the flexor tendon. The distal articular surface (Fig. 7: blue) is much more extended posteriorly in *P. guinazui* than in *Pteranodon*. The MDT of *Pteranodon* bears several small and large foramina between the proximal and distal articular surfaces. In *P. guinazui,* there is a single large foramen in the middle of the posterior area.

Bennett (2001a) described the overlap pattern of the proximal ends of the metatarsals (MTs) of *Pteranodon* as MT IV over III over II over I, but stated that other authors suggested the opposite, which "makes sense with a pterosaur foot directly derived from a crurotarsal plantigrade morphology". He also indicated that he has been "unable to find any specimens that shows [his reconstruction] is incorrect", and that "More work is needed on this problem" (Bennett 2001a: 111). Other observations in Pterosauria, as in the Azhdarchoidea (Frey et al. 2011: figs. 3, 4), and in close relatives of pterosaurs, like *Lagerpeton chanarensis* (Sereno and Arcucci 1994: fig. 3d), show the overlap pattern of the proximal ends of the MTs as I over II over III over IV. Nevertheless, for *P. guinazui*, the overlap pattern of the proximal ends of the MTs is similar to the observation of Bennett (2001a) in *Pteranodon*. In each case, the overlap pattern is accompanied by an associated beveling at the proximal end of the MTs. However, other pterosaurs, such as the Triassic taxa described by Dalla-Vecchia (2003) or the *Dimorphodon* described by Padian (1983), do not specifically show an overlap pattern. On the distal tarsals of *Dimorphodon* in distal view, a series of grooves mark where the distal tarsals receive MTs II to IV, and these are oriented anteroposteriorly, suggesting that they did not overlap proximally. The overlap pattern may have been quite variable in Pterosauria. In posterior view (plantar view for other authors), "long narrow scars on the proximal half of the posterior surface of the MTs" were observed in *Pteranodon* (Bennett 2001a: 111). Here, we observe such scars, extending along the posterior surface from the proximal depression of the MTs to the distal depression (Fig. 8A, F). In late pterodactyloids, as in Azhdarchidae and Nyctosauridae, the base of MT V overlaps the MT IV (Frey et al. 2006, 2011), a condition very different from what we observe in *P. guinazui*. The bases of the two MTs cannot overlap in *P. guinazui*, because MT V articulates with the lateral part of the LDT, unlike MT IV.

In all Triassic and most Early Jurassic pterosaurs, the MTs are arranged in a "block" (unspread), as documented by Owen (1870), Plieninger (1895), Arthaber (1919), Wellnhofer (1974), Padian (1983), Dalla Vecchia (2003), and as occurs in *Dimorphodon macronyx* (YPM350) and *Eudimorphodon*

ranzii (MCSNB 8950). This is not the case for some of the Late Jurassic pterosaurs, such as *Pterodactylus* and *Rhamphorhynchus* (Dalla Vecchia 2003). The possibility of a spread-out arrangement of the metatarsals is also supported by the triangular shape of the *Pteraichnus*-like footprint (Lockley et al. 1995; Unwin 1996; Bennett 1997; Dalla Vecchia 2003). Also, numerous studies have shown that the lateral and medial sides of pterosaur metatarsals are beveled so as to articulate tightly with their neighbors (Bennett 2001a). In *P. guinazui*, the MTs are preserved spread out (Figs. 1, 6, 8). MT I to VI lateral and medial beveling is only visible on the proximal ends of the MTs, as if the overlap occured only in their proximal part. And if the articulation of the distal tarsals is asymmetrical as proposed above, it seems that the MTs articulating with the MDT did not always move with the same amplitude as those articulating with the LDT.

Traces of what could correspond to soft tissues (Chiappe et al. 2004; Codorniú et al. 2013, 2016) can be seen between MTs I to IV (Fig. 10). Using laser fluorescence, Pittman et al. (2022) demonstrated that an aurorazhdarchid (MB.R.3531a), a close relative of the Ctenochasmatidae, had webbed feet (Pittman et al. 2022: fig. 3), which must be an adaptation to an aquatic environment. Also, Frey (2003) described webbing between the phalanges of digits *I* to *IV* in *Rhamphorhynchus muensteri* (JME SOS 4785). In extant birds, all species that depend on aquatic environments have either very long digits, webbed feet or both. As *P. guinazui* was a filter-feeder (Cerda and Codorniú 2023), it must have fed in aquatic environments (Chiappe et al. 1998; Codorniú et al. 2013). The digits of *P. guinazui* are relatively short. Moreover, the movements permitted by the ankle joint seem to correspond to those observed in the webbed feet swimming birds (Clifton and Biewener 2018). Thus, the principle of actualism suggests that *P. guinazui* could have had a webbed foot, something that has been demonstrated among other pterosaurs (Frey 2003; Pittman et al. 2022). Today, however, there is no direct evidence of webbing in *P. guinazui*. It would be interesting to use the laser fluorescence on *P. guinazui* to assess the presence of webbing between the pedal digits.

Conclusions

This work presents the first detailed study of the ankle joint of *Pterodaustro guinazui*. Some features seem to be common to all pterosaurs, others reflect its basal position in Pterodactyloidea, and some of them represent autapomorphies.

As it can been observed in Pterosauria, in the youngest specimens, the proximal tarsals are not fused to the tibia; in the subadults, the tibiotarsus is formed, but with the suture still visible; in the adults, the tibiotarsus is entirely formed, without any suture. A literature review, along with our observations on *Pterodaustro*, seems to indicate that in pterosaurs, the fusion between astragalus and calcaneum precedes tibiotarsal fusion, but that those two events occurred in close succession in the sequence of ontogenetic events, even if this fusion cannot be directly related to ontogenetic age. Only described before in *Anhanguera piscator* among pterosaurs, the medial condyle and the intercondylar groove of the tibiotarsus are made up of the astragalus, whereas the lateral condyle is composed of the calcaneum and part of the astragalus. Comparisons with other pterosaurs suggest that the overlap pattern of the pterosaurs may have been quite variable in Pterosauria, *P. guinazui* presenting a similar condition to what can be observed in *Pteranodon*, which presents a different overlapping pattern than *Azhdarcho* and *Dimorphodon*.

A bibliographical review documents that several fossils of early pterosaurs retain discrete distal tarsals II and III, whereas in the specimens of late pterodactyloids, those two bones are always fused to form the MDT. In *P. guinazui*, some specimens present unfused distal tarsals II and III, as in some other basal pterodactyloids (*Balaenognathus maeuseri*, *Ctenochasma elegans*, and one specimen of *Pterodactylus antiquus*), but others, presumably more mature individuals, present a MDT. Also, the LDT of *P. guinazui* is thicker than in *Peteinosaurus zambelli* or *Dimorphodon macronyx*, but it shares its waisted shape with those taxa. By contrast, the late pterodactyloids *Pteranodon* and *Tapejara* have their LDT with a more robust shape.

Some features of the ankle joint of *P. guinazui* are atypical of pterosaurs. On the tibiotarsus, there is a third articular facet, delimited proximo-distally by two ridges. These ridges are formed by the astragalus and the tibia, thus implying the participation of the tibia in the meso-tarsal articulation. This third articular surface appears to restrict rotation of the MDT, while the shape of the LDT allows for a rotation of great amplitude. The lateral condyle of the tibiotarsus is large, rounded, and its oblique main axis keeps the LDT in contact with the MDT through extensive flexion and extension of the ankle joint. This structure has never been described before in the literature, and may be linked to wading behavior. Also, the presence of sediment that we interpret as preservation of much-degraded remains of soft tissues between the metatarsals is documented here, possibly the remnants of what were once skin, muscles, nerves, blood vessels and, probably, a combination of these.

Acknowledgements

This research was financed by the CyT N°P-030520 project of the Universidad Nacional de San Luis (to LC), an IEA grant from the CNRS, and the Consejo Nacional de Investigaciones Científicas y Técnicas (CONICET). The constructive comments of Kevin Padian (University of California, Berkeley, USA) and an anonymous reviewer have greatly improved this manuscript. We are also grateful to Daniel E. Barta (Oklahoma State University, Tahlequah, USA) for editorial work on our manuscript.

References

Abourachid, A. and Höfling, E. 2012. The legs: a key to bird evolutionary success. *Journal of Ornithology* 153 (S1): 193–198.

Andres, B. 2021. Phylogenetic systematics of *Quetzalcoatlus* Lawson 1975 (Pterodactyloidea: Azhdarchoidea). *Journal of Vertebrate Paleontology* 41 (Supplement 1): 203–217.

Arthaber, G. von 1919. Studien über Flugsaurier auf Grund der Bearbeitung des Wiener Exemplares von *Dorygnathus banthensis* Theod. sp. *Denkschriften der Kaiserlichen Akademie der Wissenschaften/Mathematisch-Naturwissenschaftliche Classe* 97: 391–464.

Averianov, A.O. 2010. The osteology of *Azhdarcho lancicollis* Nessov, 1984 (Pterosauria, Azhdarchidae) from the late Cretaceous of Uzbekistan. *Proceedings of the Zoological Institute RAS* 314 (3): 264–317.

Beccari, V., Pinheiro, F.L., Nunes, I., Anelli, L.E., Mateus, O., and Costa, F.R. 2021. Osteology of an exceptionally well-preserved tapejarid skeleton from Brazil: Revealing the anatomy of a curious pterodactyloid clade. *PLOS ONE* 16 (8): e0254789.

Bennett, S.C. 1993. The ontogeny of *Pteranodon* and other pterosaurs. *Paleobiology* 19: 92–106.

Bennett, S.C. 1995. A statistical study of *Rhamphorhynchus* from the Solnhofen Limestone of Germany: year-classes of a single large species. *Journal of Paleontology* 69: 569–580.

Bennett, S.C. 1996. Year-classes of pterosaurs from the Solnhofen Limestone of Germany: taxonomic and systematic implications. *Journal of Vertebrate Paleontology* 16: 432–444.

Bennett, S.C. 1997. Terrestrial locomotion of pterosaurs: a reconstruction based on *Pteraichnus* trackways. *Journal of Vertebrate Paleontology* 17: 104–113.

Bennett, S.C. 2000. Pterosaur flight: The role of actinofibrils in wing function. *Historical Biology* 14: 255–284.

Bennett, S.C. 2001a. The osteology and functional morphology of the Late Cretaceous pterosaur *Pteranodon* Part I. General description of osteology. *Palaeontographica Abteilung A* 260: 1–112.

Bennett, S.C. 2001b. The osteology and functional morphology of the Late Cretaceous pterosaur *Pteranodon* Part II. Size and functional morphology. *Palaeontographica Abteilung A* 260: 113–153.

Bennett, S.C. 2007. A second specimen of the pterosaur *Anurognathus ammoni*. *Paläontologische Zeitschrift* 81: 376–398.

Bennett, S.C. 2018. New smallest specimen of the pterosaur *Pteranodon* and ontogenetic niches in pterosaurs. *Journal of Paleontology* 92: 254–271.

Bonaparte, J.F. 1970. *Pterodaustro guiñazui* gen. et sp. nov. Pterosaurio de la Formación Lagarcito, Provincia de San Luis, Argentina y su significado en la geología regional (Pterodactylidae). *Acta Geológica Lilloana* 10 (10): 207–226.

Buckland, W. 1829. On the discovery of a new species of pterodactyle in the Lias at Lyme Regis. *Transactions of the Geological Society of London* 3 (1), 217–222.

Cai, Z. and Wei, F. 1994. On a new pterosaur (*Zhejiangopterus linhaiensis* gen. et sp. nov.) from Upper Cretaceous in Linhai, Zhejiang, China. *Vertebrata PalAsiatica* 32 (3): 181.

Cerda, I.A. and Codorniú, L. 2023. Palaeohistology reveals an unusual periodontium and tooth implantation in a filter-feeding pterodactyloid pterosaur, *Pterodaustro guinazui*, from the Lower Cretaceous of Argentina. *Journal of Anatomy* 243: 579–589.

Cheng, X., Jiang, S., Wang, X., and Kellner, A.W. 2017. New anatomical information of the wukongopterid *Kunpengopterus sinensis* Wang et al., 2010 based on a new specimen. *PeerJ* 5: e4102.

Chiappe, L.M., Codorniú, L., Grellet-Tinner, G., and Rivarola, D. 2004. Argentinian unhatched pterosaur fossil. *Nature* 432: 571–572.

Chiappe, L.M., Rivarola, D., Cione, A., Fregenal-Martínez, M., Sozzi, H., Buatois, L., Gallego, O., Laza, J., Romero, E., López-Arbarello, A., Buscalioni, A., Marsicano, C., Adamonis, S., Ortega, F., McGehee, S., and Di Iorio, O. 1998. Biotic association and palaeoenvironmental reconstruction of the "Loma del *Pterodaustro*" fossil site (Early Cretaceous, Argentina). *Geobios* 31: 349–369.

Clifton, G.T. and Biewener, A.A. 2018. Foot-propelled swimming kinematics and turning strategies in common loons. *Journal of Experimental Biology* 221 (19): jeb168831.

Codorniú, L. and Chiappe, L.M. 2004. Early juvenile pterosaurs (Pterodactyloidea: *Pterodaustro guinazui*) from the Lower Cretaceous of central Argentina. *Canadian Journal of Earth Sciences* 41: 9–18.

Codorniú, L., Chiappe, L.M., and Cid, F.D. 2013. First occurrence of stomach stones in pterosaurs. *Journal of Vertebrate Paleontology* 33: 647–654.

Codorniú, L., Chiappe, L.M., and Rivarola, D. 2018. Neonate morphology and development in pterosaurs: evidence from a Ctenochasmatid embryo from the Early Cretaceous of Argentina. *Geological Society, London, Special Publications* 455: 83–94.

Codorniú, L., Paulina-Carabajal, A., and Gianechini, F.A. 2016. Braincase anatomy of *Pterodaustro guinazui*, pterodactyloid pterosaur from the Lower Cretaceous of Argentina. *Journal of Vertebrate Paleontology* 36 (1): e1031340.

Currie, P.J. and Jacobsen, A.R. 1995. An azhdarchid pterosaur eaten by a velociraptorine theropod. *Canadian Journal of Earth Sciences* 32: 922–925.

Dalla Vecchia, F.M. 1998. New observations on the osteology and taxonomic status of *Preondactylus buffarinii* Wild, 1984 (Reptilia, Pterosauria). *Bolletino della Società Paleontologica Italiana* 36: 355–366.

Dalla Vecchia, F.M. 2003. New morphological observations on Triassic pterosaurs. *Geological Society, London, Special Publications* 217: 23–44.

Dalla Vecchia, F.M. 2009. Anatomy and systematics of the pterosaur *Carniadactylus* gen. n. *rosenfeldi* (Dalla Vecchia, 1995). *Rivista Italiana di Paleontologia e stratigrafia* 115: 159–186.

Dalla Vecchia, F.M. 2021. A revision of the anatomy of the Triassic Pterosaur *Austriadraco dallavecchiai* Kellner, 2015 and of its diagnosis. *Rivista Italiana di Paleontologia e Stratigrafia* 127 (2): 427–452.

David, L.D.O., Riga, B.J.G., and Kellner, A.W. 2022. *Thanatosdrakon amaru*, gen. et sp. nov., a giant azhdarchid pterosaur from the Upper Cretaceous of Argentina. *Cretaceous Research* 137: 105228.

Dong, Z. 1982. A new pterosaur (*Huanhepterus quingyangensis* gen. et sp. nov.) from Ordos, China. *Vertebrata PalAsiatica* 20: 115–121.

Frey, E., Buchy, M.-C., Stinnesbeck, W., Gonzalez, A.G., and Di Stefano, A. 2006. *Muzquizopteryx coahuilensis* ng, n. sp., a nyctosaurid pterosaur with soft tissue preservation from the Coniacian (Late Cretaceous) of northeast Mexico (Coahuila). *Oryctos* 6 (19): e40.

Frey, E., Meyer, C.A., and Tischlinger, H. 2011. The oldest azhdarchoid pterosaur from the Late Jurassic Solnhofen Limestone (Early Tithonian) of Southern Germany. *Swiss Journal of Geosciences* 104 (S1): 35–55.

Frey, E., Tischlinger, H., Buchy, M.C., and Martill, D.M. 2003. New specimens of Pterosauria (Reptilia) with soft parts with implications for pterosaurian anatomy and locomotion. *Geological Society, London, Special Publications* 217: 233–266.

Hone, D.W., Fitch, A.J., Ma, F., and Xu, X. 2020. An unusual new genus of istiodactylid pterosaur from China based on a near complete specimen. *Palaeontologia Electronica* 23 (1): 1–43.

Hone, D.W., Habib, M.B., and Therrien, F. 2019. *Cryodrakon boreas*, gen. et sp. nov., a Late Cretaceous Canadian azhdarchid pterosaur. *Journal of Vertebrate Paleontology* 39 (3): e1649681.

Hone, D.W., Tischlinger, H., Frey, E., and Röper, M. 2012. A new non-pterodactyloid pterosaur from the Late Jurassic of Southern Germany. *PLoS ONE* 7 (7): e39312.

Jenkins, F.A., Jr., Shubin, N.H., Gatesy, S.M., and Padian, K. 2001. A diminutive pterosaur (Pterosauria: Eudimorphodontidae) from the Greenlandic Triassic. *Bulletin of the Museum of Comparative Zoology* 156: 151–170.

Ji, S.-A. and Ji, Q. 1997. Discovery of a new pterosaur in western Liaoning, China. *Acta Geologica Sinica-English Editio*n 71: 115–121.

Ji, S.-A. and Ji, Q. 1998. A new fossil pterosaur (Rhamphorhynchoidea) from Liaoning, *Dendrorhynchus curvidentatus*, gen. et sp. nov. *Jiangsu Geology* 22 (4): 199–206.

Kellner, A.W.A. 2003. Pterosaur phylogeny and comments on the evolutionary history of the group. *Geological Society, London, Special Publications* 217: 105–137.

Kellner, A.W.A. 2004. The ankle structure of two pterodactyloid pterosaurs from the Santana Formation (Lower Cretaceous), Brazil. *Bulletin of the American Museum of Natural History* 2004 (285): 25–35.

Kellner, A.W. 2015. Comments on Triassic pterosaurs with discussion about ontogeny and description of new taxa. *Anais da Academia Brasileira de Ciências* 87: 669–689.

Kellner, A.W. and Tomida, Y. 2000. Description of a new species of Anhangueridae (Pterodactyloidea) with comments on the pterosaur fauna from the Santana Formation (Aptian–Albian), northeastern Brazil. *National Science Museum Monographs* 17: ix–137.

Kellner, A.W., Caldwell, M.W., Holgado, B., Vecchia, F.M.D., Nohra, R., Sayão, J.M., and Currie, P.J. 2019. First complete pterosaur from the Afro-Arabian continent: insight into pterodactyloid diversity. *Scientific Reports* 9 (1): 17875.

Laurin, M. and Germain, D. 2011. Developmental characters in phylogenetic inference and their absolute timing information. *Systematic Biology* 60: 630–644.

Laurin, M., Lapauze, O., and Marjanović, D. 2022. What do ossification sequences tell us about the origin of extant amphibians? *Peer Community Journal* 2: e12.

Lockley, M.G., Logue, T.J., Moratalla, J.J., Hunt, A.P., Schultz, R.J., and Robinson, J.W. 1995. The fossil trackway *Pteraichnus* is pterosaurian, not crocodilian: Implications for the global distribution of pterosaur tracks. *Ichnos* 4: 7–20.

Longrich, N.R., Martill, D.M., and Andres, B. 2018. Late Maastrichtian pterosaurs from North Africa and mass extinction of Pterosauria at the Cretaceous–Paleogene boundary. *PLoS Biology* 16 (3): e2001663.

Lü, J. 2003. A new pterosaur: *Beipiaopterus chenianus*, gen. et sp. nov. (Reptilia: Pterosauria) from western Lianong Province of China. *Memoir of the Fukui Prefectural Dinosaur Museum* 2: 153.

Lü, J. 2009. A new non-pterodactyloid pterosaur from Qinglong County, Hebei Province of China. *Acta Geologica Sinica-English Edition* 83: 189–199.

Lü, J. 2010. A new boreopterid pterodactyloid pterosaur from the Early Cretaceous Yixian Formation of Liaoning Province, northeastern China. *Acta Geologica Sinica-English Edition* 84: 241–246.

Lü, J. and Ji, Q. 2005a. A new ornithocheirid from the Early Cretaceous of Liaoning Province, China. *Acta Geologica Sinica-English Edition* 79: 157–163.

Lü, J. and Ji, Q. 2005b. New azhdarchid pterosaur from the Early Cretaceous of western Liaoning. *Acta Geologica Sinica-English Edition* 79: 301–307.

Lü, J., Meng, Q., Wang, B., Liu, D., Shen, C., and Zhang, Y. 2018. Short note on a new anurognathid pterosaur with evidence of perching behaviour from Jianchang of Liaoning Province, China. *Geological Society, London, Special Publications* 455: 95–104.

Lü, J., Pu, H., Xu, L., Wei, X., Chang, H., and Kundrát, M. 2015. A new rhamphorhynchid pterosaur (Pterosauria) from Jurassic deposits of Liaoning Province, China. *Zootaxa* 3911: 119–129.

Lü, J., Unwin, D.M., Jin, X., Liu, Y., and Ji, Q. 2010. Evidence for modular evolution in a long-tailed pterosaur with a pterodactyloid skull. *Proceedings of the Royal Society B: Biological Sciences* 277: 383–389.

Lü, J., Unwin, D.M., Zhao, B., Gao, C., and Shen, C. 2012. A new rhamphorhynchid (Pterosauria: Rhamphorhynchidae) from the Middle/Upper Jurassic of Qinglong, Hebei Province, China. *Zootaxa* 3158: 1–19.

Lü, J., Xu, L., Chang, H., and Zhang, X. 2011. A new darwinopterid pterosaur from the Middle Jurassic of western Liaoning, northeastern China and its ecological implications. *Acta Geologica Sinica-English Edition* 85: 507–514.

Martill, D.M., Frey, E., Tischlinger, H., Mäuser, M., Rivera-Sylva, H.E., and Vidovic, S.U. 2023. A new pterodactyloid pterosaur with a unique filter-feeding apparatus from the Late Jurassic of Germany. *PalZ* 97 (2): 1–42.

Mayr, G. 2011. Metaves, Mirandornithes, Strisores and other novelties—a critical review of the higher-level phylogeny of neornithine birds: Higher-level phylogeny of birds. *Journal of Zoological Systematics and Evolutionary Research* 49: 58–76.

Mazin, J.-M. and Pouech, J. 2020. The first non-pterodactyloid pterosaurian trackways and the terrestrial ability of non-pterodactyloid pterosaurs. *Geobios* 58: 39–53.

Morse, E.S. 1880. *On the Identity of the Ascending Process of the Astragalus in Birds with the Intermedium. Anniversary Memoirs of the Boston Society of Natural History*. 10 pp. Boston Society of Natural History, Boston.

Naish, D., Witton, M.P., and Martin-Silverstone, E. 2021. Powered flight in hatchling pterosaurs: evidence from wing form and bone strength. *Scientific Reports* 11 (1): 13130.

Olori, J.C. 2013. Ontogenetic sequence reconstruction and sequence polymorphism in extinct taxa: an example using early tetrapods (Tetrapoda: Lepospondyli). *Paleobiology* 39: 400–428.

Ősi, A., Prondvai, E., and Géczy, B. 2010. The history of Late Jurassic pterosaurs housed in Hungarian collections and the revision of the holotype of *Pterodactylus micronyx* Meyer 1856 (a "Pester Exemplar"). *Geological Society, London, Special Publications* 343: 277–286.

Owen, P. 1870. Monograph of the fossil Reptilia of the Liassic Formations. Part Second. Pterosauria. *Monographs of the Palaeontographical Society* 23 (104): 41–81.

Padian, K. 1983. Osteology and functional morphology of *Dimorphodon macronyx* (Buckland) (Pterosauria: Rhamphorhynchoidea) based on new material in the Yale Peabody Museum. *Postilla* 189: 1–44.

Padian, K. 2008. The Early Jurassic pterosaur *Dorygnathus banthensis* (Theodori, 1830). *Special Papers in Palaeontology* 80: 69–107.

Padian, K. 2017. Structure and evolution of the ankle bones in pterosaurs and other ornithodirans. *Journal of Vertebrate Paleontology* 37 (5): e1364651.

Padian, K., Cunningham, J.R., Langston, W., Jr., and Conway, J. 2021. Functional morphology of *Quetzalcoatlus* Lawson 1975 (Pterodactyloidea: Azhdarchoidea). *Journal of Vertebrate Paleontology* 41 (Supplement): 218–251.

Piñeiro, G., Demarco, P.N., and Meneghel, M.D. 2016. The ontogenetic transformation of the mesosaurid tarsus: a contribution to the origin of the primitive amniotic astragalus. *PeerJ* 4: e2036.

Pittman, M., Barlow, L.A., Kaye, T.G., and Habib, M.B. 2021. Pterosaurs evolved a muscular wing-body junction providing multifaceted flight performance benefits: Advanced aerodynamic smoothing, sophisticated wing root control, and wing force generation. *Proceedings of the National Academy of Sciences* 118 (44): e2107631118.

Pittman, M., Kaye, T.G., Campos, H.B., and Habib, M.B. 2022. Quadrupedal water launch capability demonstrated in small Late Jurassic pterosaurs. *Scientific Reports* 12 (1): 6540.

Plieninger, F. 1895. *Campylognathus zitteli*: a new pterosaur from the Upper Lias of Swabia. *Palaeontographica: Beiträge zur Naturgeschichte der Vorzeit* 41: 193.

Romer, A.S. and Parsons, T.S. 1977. *The Vertebrate Body, Fifth Edition*. Holt-Saunders International, Philadelphia.

Schaeffer, B. 1941. The morphological and functional evolution of the tarsus in amphibians and reptiles. *Bulletin of the American Museum of Natural History* 78: article 6.

Sereno, P.C. and Arcucci, A.B. 1994. Dinosaurian precursors from the Middle Triassic of Argentina: *Lagerpeton chanarensis*. *Journal of Vertebrate Paleontology* 13: 385–399.

Shen, C., Pêgas, R.V., Gao, C., Kundrát, M., Zhang, L., Wei, X., and Zhou, X. 2021. A new specimen of *Sinopterus dongi* (Pterosauria, Tapejaridae) from the Jiufotang Formation (Early Cretaceous, China). *PeerJ* 9: e12360.

Stecher, R. 2008. A new Triassic pterosaur from Switzerland (Central Austroalpine, Grisons), *Raeticodactylus filisurensis* gen. et sp. nov. *Swiss Journal of Geosciences* 101: 185–201.

Unwin, D.M. 1996. Pterosaur tracks and the terrestrial ability of pterosaurs. *Lethaia* 29: 373–386.

Unwin, D.M. and Bakhurina, N.N. 1994. Sordes pilosus and the nature of the pterosaur flight apparatus. *Nature* 371: 62–64.

Vidovic, S.U. and Martill, D.M. 2014. *Pterodactylus scolopaciceps* Meyer, 1860 (Pterosauria, Pterodactyloidea) from the Upper Jurassic of Bavar-

ia, Germany: the problem of cryptic pterosaur taxa in early ontogeny. *PloS ONE* 9 (10): e110646.

Vidovic, S.U. and Martill, D.M. 2018. The taxonomy and phylogeny of *Diopecephalus kochi* (Wagner, 1837) and "*Germanodactylus rhamphastinus*" (Wagner, 1851). *Geological Society, London, Special Publications* 455: 125–147.

Wagner, J.A. 1861. Charakteristik einer neuen Flugeidechse, *Pterodactylus elegans*. *Sitzungsbericht der Bayerischen Akademie der Wissenschaften* 1 (17): S363–S365.

Wang, X. and Lü, Q. 2001. Discovery of a pterodactylid pterosaur from the Yixian Formation of western Liaoning, China. *Chinese Science Bulletin* 46: A3–A8.

Wang, X. and Zhou, Z. 2003. A new pterosaur (Pterodactyloidea, Tapejaridae) from the Early Cretaceous Jiufotang Formation of western Liaoning, China and its implications for biostratigraphy. *Chinese Science Bulletin* 48: 16–23.

Wang, X., Jiang, S., Zhang, J., Cheng, X., Yu, X., Li, Y., Wei, G., and Wang, X. 2017. New evidence from China for the nature of the pterosaur evolutionary transition. *Scientific Reports* 7 (1): 42763.

Wang, X., Kellner, A.W., Jiang, S., and Meng, X. 2009. An unusual long-tailed pterosaur with elongated neck from western Liaoning of China. *Anais da Academia Brasileira de Ciências* 81: 793–812.

Wang, X., Kellner, A.W., Jiang, S., Cheng, X., Meng, X., and Rodrigues, T. 2010. New long-tailed pterosaurs (Wukongopteridae) from western Liaoning, China. *Anais da Academia Brasileira de Ciências* 82: 1045–1062.

Wang, X., Kellner, A.W., Zhou, Z., and de Almeida Campos, D. 2008. Discovery of a rare arboreal forest-dwelling flying reptile (Pterosauria, Pterodactyloidea) from China. *Proceedings of the National Academy of Sciences* 105: 1983–1987.

Wang, X., Zhou, Z., Zhang, F., and Xu, X. 2002. A nearly completely articulated rhamphorhynchoid pterosaur with exceptionally well-preserved wing membranes and "hairs" from Inner Mongolia, northeast China. *Chinese Science Bulletin* 47: 226–230.

Wei, X., Pêgas, R.V., Shen, C., Guo, Y., Ma, W., Sun, D., and Zhou, X. 2021. *Sinomacrops bondei*, a new anurognathid pterosaur from the Jurassic of China and comments on the group. *PeerJ* 9: e11161.

Wellnhofer, P. 1970. Die Pterodactyloidea (Pterosauria) der Oberjura-Plattenkalke Suddentschlands. *Bayerische Akademie der Wissenschaften Mathematisch-Naturwissenschaftliche Klasse Abhandlungen Neue Folge H* 141: 1–133.

Wellnhofer, P. 1974. *Campylognathoides liasicus* (Quenstedt), an Upper Liassic pterosaur from Holzmaden – The Pittsburgh specimen. *Annals of the Carnegie Museum* 45 (2): 5–34.

Wellnhofer, P. 1975. Die Rhamphorhynchoidea (Pterosauria) der Oberjura-Plattenkalke Süddeutschlands. Teil II: Systematische Beschreibung. *Palaeontographica Abteilung A* 148: 132–186.

Wellnhofer P. 1978. Pterosauria. *In*: P. Wellnhofer (ed.), *Handbuch der Paläoherpetologie. Encyclopedia of Paleoherpetology. Vol. 19*, 1–82. Gustav Fischer, Stuttgart.

Wellnhofer, P. 1991. *Illustrated Encyclopedia of Pterosaurs*. 192 pp. Crescent Books, New York.

Winkler, T.C. 1870. *Description d'un nouvel exemplaire de* Pterodactylus micronyx *du Musée Teyler*. Archives du Musée Teyler, Vol. III, fasc. 1er. 16 pp. Les Héritiers Loosjes, Harlem.

Witton, M.P. 2015. Were early pterosaurs inept terrestrial locomotors? *PeerJ* 3: e1018.

Zambelli, R. 1973. *Eudimorphodon ranzii* gen. nov., sp. nov., uno pterosauro triassico. *Rendiconti/Istituto lombardo. B, Scienze biologiche e mediche* 107: 27.

Zeffer, A. and Norberg, U.L. 2003. Leg morphology and locomotion in birds: requirements for force and speed during ankle flexion. *Journal of Experimental Biology* 206: 1085–1097.

Zhang, X., Jiang, S., Kellner, A.W., Cheng, X., Costa, F.R., and Wang, X. 2023. A new species of *Eopteranodon* (Pterodactyloidea, Tapejaridae) from the Lower Cretaceous Yixian Formation of China. *Cretaceous Research* 149: 105573.

Zhou, C.F. 2010. New material of *Elanodactylus prolatus* Andres & Ji, 2008 (Pterosauria: Pterodactyloidea) from the Early Cretaceous Yixian Formation of western Liaoning, China. *Neues Jahrbuch fur Geologie und Palaontologie, Abhandlungen* 255: 277.

Zhou, C.-F., Wang, X., and Wang, J. 2022. First evidence for tooth—tooth occlusion in a ctenochasmatid pterosaur from the Early Cretaceous Jehol Biota. *Geological Society, London, Special Publications* 521: 9–17.

Zhou, X., Pêgas, R.V., Ma, W., Han, G., Jin, X., Leal, M.E., and Shen, C. 2021. A new darwinopteran pterosaur reveals arborealism and an opposed thumb. *Current Biology* 31: 2429–2436.